

# Single or Multiple Frames Content Delivery for Robust and Secure Communication in Energy and Spectrum Efficient 5G Networks?

Mohammad R. Abedi, Mohammad R. Javan, Nader Mokari

## Abstract

This paper addresses the four enabling technologies, namely multi-user sparse code multiple access (SCMA), content caching, energy harvesting, and physical layer security for proposing an energy and spectral efficient resource allocation algorithm for the access and backhaul links in heterogeneous cellular networks. Although each of the above mentioned issues could be a topic of research, in a real situation, we would face a complicated scenario where they should be considered jointly, and hence, our target is to consider these technologies jointly in a unified framework. Moreover, we propose two novel content delivery scenarios: 1) single frame content delivery, and 2) multiple frames content delivery. In the first scenario, the requested content by each user is served over one frame. However, in the second scenario, the requested content by each user can be delivered over several frames. We formulate the resource allocation for the proposed scenarios as optimization problems where our main aim is to maximize the energy efficiency of access links subject to the transmit power constraints of access and backhaul links, caching and energy harvesting constraints, and SCMA codebook allocation limitations. Due to the practical limitations, we assume that the channel state information values between eavesdroppers and base stations are uncertain and design the network for the worst case scenario. Since the corresponding optimization problems are mixed integer non-linear and nonconvex programming, NP-hard, and intractable, we propose an iterative algorithm based on the well-known alternative and successive convex approximation methods. In addition, the proposed algorithms are studied from the computational complexity, convergence, and performance perspectives. Moreover, the proposed caching scheme outperforms the existing traditional caching schemes like random caching and most popular caching. we also study the effect of joint and disjoint considerations of enabling technologies for the performance of 5G networks.

**Index Terms**— Heterogeneous cellular networks, Content caching, Physical layer security, Energy harvesting, Imperfect CSI.

## I. INTRODUCTION

### A. *Backgrounds and Motivations*

Over recent years, the growth of high data rate of mobile traffic, energy, content storing, security, and limited knowledge of channels over mobile networks are the major challenges of network designing and implementation. To tackle these issues and cope with the users' requirements, fifth-generation (5G) of wireless communications is introduced which uses multiple advanced techniques such as energy harvesting (EH), physical layer (PHY) security, new multiple access techniques, and content caching. Hence, all of these issues must be considered together and efficient radio resource allocation algorithms and content placement must be used to provide high performance for the designed networks. However, devising efficient radio resource allocation algorithms to handle all these issues is a challenging work, and to the best our knowledge, no research exists addressing all these issues together in a unified framework. Although each of the mentioned issues could be an interesting research topic, our main contribution is to study the joint effect of security, EH, content caching, and imperfect and the limited channel knowledge in a unified joint access and backhaul links framework. In this regards, we develop a comprehensive model and mathematical representation, and design a robust resource allocation algorithm. Although the resulting optimization problem is much complicated, effective optimization methods are used to achieve the solution of the optimization problem. The outline of each issue, applicable solutions, and related works are explained in the sequel.

1) *Growth of High data Rate Mobile Traffic*: Incredible growth in high data rate mobile applications requires high capacity in radio access and backhaul wireless links. However, the centralized nature of mobile network architectures can not provide enough capacity on the wireless access and backhaul links to satisfy high demand for rich multimedia content requirements. Heterogeneous networks is a promising solution to improve coverage and to provide high capacity.

2) *Content Caching*: Multimedia services can be achieved using recent advanced mobile communication technologies by new types of mobile devices such as smart phones and tablets. However, transferring the same content several times in a short periods imposes capacity pressures on the network. To overcome this, content caching at the network edge has recently been emerged

as a promising technique in 5G networks. Caching in 5G mobile networks also reduces the mobile traffic by eliminating the redundant traffic of duplicate transmissions of the same content from servers. The deployment of content caching relevant to evolved packet core and radio access network (RAN) are studied in [1]. By caching, contents can be closer to the end-users, and backhaul traffic can be offloaded [2] to the edge of the network. The authors in [3], [4] investigate caching the contents in RAN with the aim to store contents closer to users. The content caching in small-cell base stations is studied in [4], [5].

3) *Energy Harvesting*: Design of high-rate services increases the energy consumption at receivers which degrades the battery life. Therefore, trade-off between high-rate requirement and long battery life is required to achieve good performance. Energy harvesting has emerged as a promising approach to provide sustainable networks with the long-term sustainable operation of power supplies. In EH communication networks, nodes acquire energy from environmental energy sources including random motion and mechanical vibrations, light, acoustic, airflow, heat, RF radio waves [6], [7]. Design of novel transmission policies due to highly random and unpredictable nature of harvestable profile of the harvested energy is required which would be a challenging task.

4) *New Multiple Access Techniques*: Sparse code multiple access (SCMA) with near optimal spectral efficiency is a promising technique to improve capacity of wireless radio access [8]. This multiple-access technique that is based on non-orthogonal codebook assignment provides massive connectivity and improves spectral efficiency [8], [9]. By performing an appropriate codebook assignment, a subcarrier in SCMA networks can be shared among multiple users. Joint codebook assignment and power allocation for SCMA is studied in [10]. The codebook assignment and power allocation is also investigated in [11]. The authors formulate energy-efficient transmission problem to maximize the network energy efficiency (EE) subject to system constraints.

5) *Imperfect Channel State Information*: In the most previous works, the authors assume perfect channel state information (CSI) of all links for BSs. However, in practice, knowing of perfect CSI in BSs requires a huge amount of bandwidth for signalling through the feedback links which is not possible. Moreover, due to time varying channel, feedback delay, quantization error, and estimation errors, perfect CSI may not be available at transmitters. In this regard, some works aim to tackle the performance degradation caused by the limited and imperfect CSI [12]–[14]. In [12], the authors investigate the power and subcarrier allocation by the quantized CSI. It is assumed that the perfect CSI does not exist at transmitters and imperfect CSI can be achieved

via limited rate feedback channels. In [13], joint power and subcarrier allocation is studied for the uplink of an orthogonal frequency-division multiple access (OFDMA) heterogeneous wireless network (HetNet) assuming imperfect CSI. In [14], a limited rate feedback scheme is considered to maximize the average achievable rate for decode-and-forward relay cooperative networks.

6) *Security*: The broadcast nature of wireless transmission makes security against eavesdropping a major challenge for the next generation wireless networks [15]. In this regards, physical-layer security is a promising method to provide security in wireless networks [16], [17]. This technique explores the characteristics of the wireless channel to provide security for wireless transmission. In [18], the authors consider physical layer security for relay assisted networks with multiple eavesdroppers. They maximize the sum secrecy rate of network with respect to transmission power constraint for each transmitter via imperfect CSI. In [19], the authors investigate the benefits of three promising technologies, i.e., physical layer security, content caching, and EH in heterogeneous wireless networks.

7) *Joint Backhaul and Access Resource Allocation*: Joint resource allocation at backhaul and access links is investigated in [20] for heterogeneous networks. In [20], the full duplex self-backhauling capacity is used to simultaneously communicate over the backhaul and access links. In [21], joint access and backhual links optimization is considered to minimize the total network power consumption. In [22], the authors study joint wireless backhaul and the access links resource allocation optimization. The goal is to maximize the sum rate subject to the backhaul and access constraints. Joint backhaul and access links optimization is considered in [23] for dense small cell networks. Joint resource allocation in access and backhaul links is considered for ultra dense networks in [24] where the goal is to maximize the throughput of the network under system constraints. In [25], the authors consider joint access and backhaul resource allocation for the admission control of service requests in wireless virtual network. The access and backhaul links optimization are considered for small cells in the mmW frequency in [26].

## B. Our Contributions

This paper addresses the above joint provisioning of resources between the wireless backhauls and access links by using multi-user SCMA (MU-SCMA) to improve the network energy efficiency. We consider secure communications in EH enabled SCMA downlink communications with imperfect channel knowledge. In our work, we consider several techniques to improve

performance of network and formulate an optimization problem with the aim of maximizing EE with respect to system constraints. There are several works which consider each of these topics separately. However, in a real situation, these issues should be considered jointly which is a complicated scenario. To the best of our knowledge, none of the existing works considered the above issues in a unified framework. The main contributions of this work are as follows:

- We provide a unified framework in which physical layer security, content caching, EH, and imperfect knowledge of channel information is considered jointly in the design of wireless communication networks
- We consider SCMA as a non-orthogonal multiple access technology where the codebooks are allowed to be used several times among users which increases the spectral efficiency.
- We propose two novel different scenarios for content delivery, namely single frame content delivery (SFCD), and multiple frames content delivery (MFCD). We compare the performance of the proposed delivery scenarios with each other for different system parameters. Due to the random energy arrivals in the EH based communication, there may not be enough energy to send the entire file at the desired . Therefore, the first scenario may interrupt sending the file. To overcome this difficulty, we can use the second scenario. In this scenario, due to the file transfer in multiple slots, the probability of interrupting will be very low. It should be noted that the second scenario can be suitable for applications with large file sizes.
- We consider the access and backhaul links jointly and formulate the resource allocation for the proposed scenarios as optimization problems whose objectives are to maximize the energy efficiency of the network while transmit power constraints, EH constraints, codebook assignment constraints, as well as caching constraints should be satisfied.
- We provide mathematical frameworks for our proposed resource allocation problems where fractional programming, alternative optimization, and successive convex approximation method are used to achieve solutions for the resource allocation optimization problems. We further study the convergence and the computational complexity of the proposed resource allocation algorithms.
- We evaluate the performance of the proposed scheme for different values of the network parameters using simulations.

## II. SYSTEM MODELS

Consider the downlink SCMA transmission of a wireless heterogenous cellular network comprising of  $O$  macro base stations (MBSs) and  $J$  small base stations (SBSs) in a two dimensional Euclidean plane  $\mathbb{R}^2$ , as shown in Fig. 1. Let us denote by  $\mathcal{O} = \{1, 2, \dots, O\}$  the set of the MBSs and by  $\mathcal{J} = \{1, 2, \dots, J\}$  the set of the SBSs. Each cache-capable base station, i.e.,  $b \in \mathcal{B} = \{1, \dots, B\} = \mathcal{O} \cup \mathcal{J}$  with size  $B = |\mathcal{B}|$ , is connected to core network via backhaul<sup>1</sup> links which are wireless links. The paper assumes that there is no interference between the wireless backhaul and access links and these links are out-of-band. A set of total number of users,  $\mathcal{U}_b = \{1, 2, \dots, U_b\}$  is served by base station  $b$  with size  $U_b = |\mathcal{U}_b|$ . The set of network users is  $\mathcal{U} = \bigcup_{b=1}^B \mathcal{U}_b$ . The system consists of  $Q$  eavesdroppers which are indexed by  $q \in \mathcal{Q} = \{1, 2, \dots, Q\}$  with size  $Q = |\mathcal{Q}|$ . The total transmit bandwidth of the access, i.e., BW, is divided into  $N$  subcarriers where the bandwidth of each subcarrier is  $BW_n$  ( $BW = N \times BW_n$ ).  $K$  social media  $\omega_k, k \in \mathcal{K} = \{1, \dots, K\}$ , as the main traffic of internet contents, are requested by the users in the network. We assume that during the runtime of the network optimization process, user-BS association is fixed. An SCMA encoder is used to map  $\log_2(Z)$  bits to an

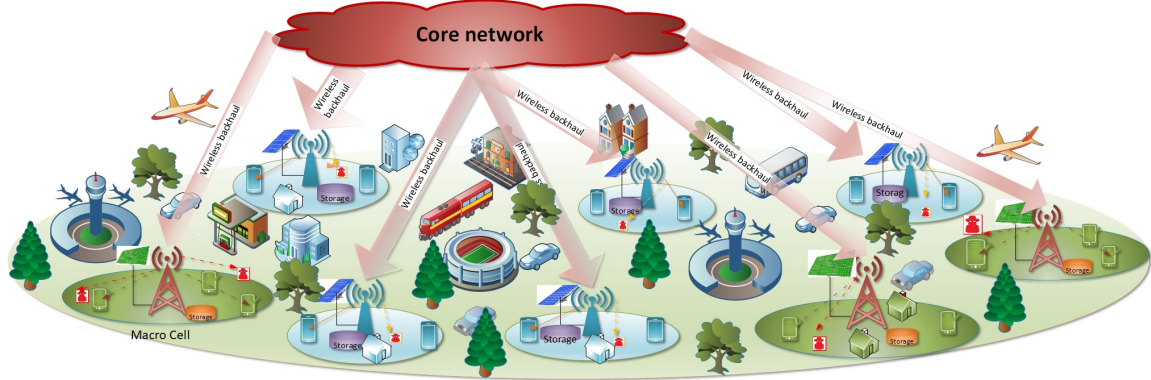


Fig. 1. A schematic of the system model.

$N$ -dimensional complex codebook of size  $Z$  [8]. Corresponding to  $\Pi$  specific subcarriers, there are  $N$ -dimensional complex codewords of a codebook which are sparse vectors with  $\Pi$  ( $\Pi < N$ ) non-zero entries. The mapping between codebooks and subcarriers is done using a set of indicator variables  $\{c_{nm}\}$ , where  $c_{nm} = 1$  if codebook  $m$  occupies subcarrier  $n$ , otherwise  $c_{nm} = 0$ . There

<sup>1</sup>Point-to-multipoint (PMP) technologies is considered as backhaul networks for small cell which is an effective way of sharing the backhaul resource between several BSs. PMP backhaul has high spectral efficiency, and speed and flexibility of deployment, and have been successfully deployed in the Middle East, Africa and in Europe by major operators [27].

are  $M$  codebooks. The message passing algorithm (MPA) can be used to detect multiplexed signals on the same subcarriers [28].

We assume that the time is split into several super frames where over each super frame the request of users should be served and the proposed content caching and resource allocation algorithms are run over each super frame. We further assume that each super frame is divided into  $F$  frames of duration  $T$  seconds. In our resource allocation framework, we consider two tasks: content caching and delivery resource allocations. The content caching task deals with determining which content should be cached in which storage. However, the delivery task deals with performing resource allocation such that the contents are delivered to the requesting users within  $F$  frames. At the beginning of each super frame, if a change in the content popularity stochastic is detected, joint content caching and radio resource allocation is performed, and otherwise, only radio resource allocation is performed. Note that the proposed resource allocation problem is solved at the beginning of each super frame, and hence, the information about the CSIs of channels and energy harvesting profile over all  $F$  frames are required and should be known in advanced. With such assumption, we rely on the off-line approach which is common in the context of energy harvesting<sup>2</sup> [29], [30]. The proposed transmission structure is shown in Fig. 2.

Let  $\mathbf{s} = \{s_{bu}^{mt}\}$  denote the codebook assignment at BS  $b$  at frame  $t$  where  $s_{bu}^{mt}$  is an indicator variable that is 1 if codebook  $m$  is assigned to user  $u$  at BS  $b$  at frame  $t$  and 0 otherwise. Furthermore, let  $\mathbf{p} = \{p_{bu}^{mt}\}$  denote the allocated transmit power vector with  $p_{bu}^{mt}$  representing the transmit power for user  $u$  at BS  $b$  at frame  $t$  on codebook  $m$ . Thus, the total transmit power of BS  $b$  at frame  $t$  is  $\sum_{u \in \mathcal{U}_b} \sum_{m \in \mathcal{M}} s_{bu}^{mt} p_{bu}^{mt}, \forall b \in \mathcal{B}, t \in \mathcal{F}$ . To transmit the codewords to the designated users, the transmit power,  $\mathbf{p}$  is finally allocated on the corresponding subcarriers. However, different from OFDMA based networks, the transmit power  $p_{bu}^{mt}$  is allocated on subcarrier  $n$  according to a given proportion  $\eta_{nm}$ , which is determined by the codebook design ( $0 < \eta_{nm} < 1$  when  $c_{nm} = 1$  and  $\eta_{nm} = 0$  when  $c_{nm} = 0$  [8]). Therefore, the signal-to-interference-plus-noise

<sup>2</sup>In the context of energy harvesting, there is another approach which is called on-line approach. The approach assumes that the information is available only causally and use the Markov decision process method for resource allocation over  $F$  frames [30]. Although the availability of noncausal information is no practical, the off-line approach would provide a benchmark for energy harvesting networks. We leave the on-line approach as a future research direction

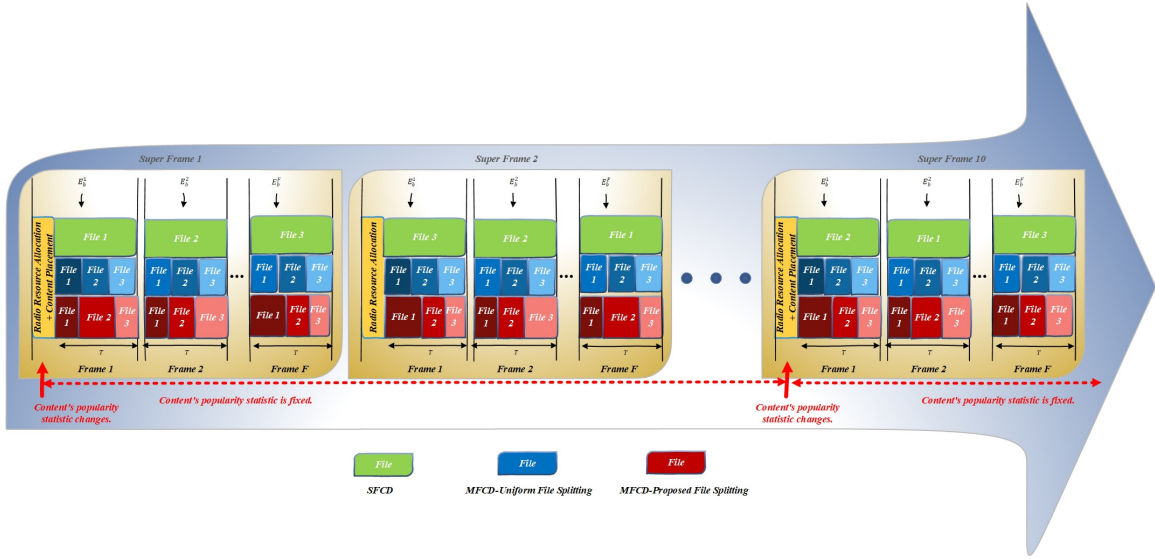


Fig. 2. SFCD and MFCD transmission structure.

ratio (SINR) of user  $u$  in BS  $b$  when using codebook  $m$  can be expressed as follows:

$$\gamma_{bu}^{mt} = \frac{\sum_{n \in \mathcal{N}} \eta_{nm} s_{bu}^{mt} p_{bu}^{mt} g_{bu}^{nt}}{I_{bu}^{mt} + (\sigma_u^n)^2}, \quad (1)$$

where  $I_{bu}^{mt} = \sum_{b \in \mathcal{B} \setminus \{b\}} \sum_{u \in \mathcal{U}_b} \sum_{n \in \mathcal{N}} \eta_{nm} s_{bu}^{mt} p_{bu}^{mt} g_{bu}^{nt}$  and  $g_{bu}^{nt}$  denotes the channel power gains between BS  $b$  and user  $u$  on subcarrier  $n$  at time  $t$ . Each of the subcarriers can be assumed to undergo a flat-fading, and hence, the channel coefficients are kept constant within each frame. The achievable rate for the  $u^{\text{th}}$  user in BS  $b$  at frame  $t$  on codebook  $m$  is given by  $R_{bu}^{D,mt} = \log_2 (1 + \gamma_{bu}^{mt})$ . As such, the SINR of eavesdropper  $q$  in BS  $b$  when using codebook  $m$  can be expressed as:

$$\hat{\gamma}_{buq}^{mt} = \frac{\sum_{n \in \mathcal{N}} \eta_{nm} s_{bu}^{mt} p_{bu}^{mt} h_{bq}^{nt}}{\hat{I}_{buq}^{mt} + (\sigma_q^n)^2}, \quad (2)$$

where  $\hat{I}_{buq}^{mt} = \sum_{b \in \mathcal{B} \setminus \{b\}} \sum_{u \in \mathcal{U}_b} \sum_{n \in \mathcal{N}} \eta_{nm} s_{bu}^{mt} p_{bu}^{mt} h_{bq}^{nt}$  and  $h_{bq}^{mt}$  denotes the channel power gains between BS  $b$  and eavesdropper  $q$  on subcarrier  $n$ . The achievable rate for the  $q^{\text{th}}$  eavesdropper in BS  $b$  at frame  $t$  is evaluated by  $R_{buq}^{E,mt} = \log_2 (1 + \hat{\gamma}_{buq}^{mt})$ . The achievable secrecy access rate for the  $u^{\text{th}}$  user in BS  $b$  at frame  $t$  on codebook  $m$  is expressed as,

$$R_{bu}^{S,mt} = \left[ R_{bu}^{D,mt} - \max_{q \in \mathcal{Q}} R_{buq}^{E,mt} \right]^+ = \max \left\{ R_{bu}^{D,mt} - \max_{q \in \mathcal{Q}} R_{buq}^{E,mt}, 0 \right\}, \quad (3)$$

where  $[x]^+ = \max\{0, x\}$ .

### III. THE OPTIMIZATION FRAMEWORK

In this section, we provide the design objective and a characterization of the constraints that must be satisfied by content caching, EH, codebook assignment, and power allocations.

### A. System Constraints

1) *Content Caching Constraints*: Let the finite size of cache memory at the  $b^{\text{th}}$  BS is denoted by  $V_b$ . If the requested file  $k$  by user  $u$  exists in the cache, then the file is sent to user immediately. This event is referred as a cache hit. However, if file  $k$  does not exist in the cache, then the request is forwarded to the core network via backhaul, then downloaded file  $k$  from the core network via backhaul is forwarded to the user. The size of the social media,  $\alpha_k, k \in \mathcal{K}$  is assumed to be Log-Normal distributed, i.e.  $\alpha_k \sim \ln \mathcal{N}(\mu, \beta^2)$  [31]. As the total cached media should not exceed the finite size of cache memory at BS  $b$ , we have

$$\sum_{k \in \mathcal{K}} \theta_{bk} \alpha_k \leq V_b, \forall b \in \mathcal{B}, \quad (4)$$

where  $\theta_{bk}$  is a binary indicator declaring whether social media  $\omega_k$  is cached at BS  $b$ .

2) *Content Delivery*: The content delivery consists of two phases: 1) a cache placement phase, and 2) a content delivery phase. In the cache placement phase, the cache content is determined at each BS, and in the content delivery phase, the requested files are delivered to users over wireless channels. In this paper, two new delivery scenarios are considered for content delivery phase. In the first scenario, the user's requested file  $k$  with size  $\alpha_k$  is sent in a single frame, while in the second scenario the user's requested file  $k$  is divided into several parts with size  $\{\beta_k^t\}, \forall t, k$ , which are sent over several frames. The scenarios are shown in the Fig. 2. To ensure that all parts of each file is transmitted to user, the following constraint should be satisfied

$$\sum_{t \in F} \beta_k^t = \alpha_k, \forall k. \quad (5)$$

3) *Access and Backhaul Links Constraints*: Let  $v_{ku}$  denote whether user  $u$  needs  $\omega_k$ . The backhaul traffic for BS  $b$  constraint for the SFCD scenario is written as follows

$$\sum_{k \in \mathcal{K}} \sum_{u \in \mathcal{U}_b} \sum_{m \in \mathcal{M}} s_{bu}^{mt} (1 - \theta_{bk}) \cdot \min \left\{ \sum_{u \in \mathcal{U}_b} v_{ku}, 1 \right\} \alpha_k \leq \sum_{n \in \mathcal{N}} \zeta_{bn} \tilde{R}_b^{nt}, \forall t \in \mathcal{F}, b \in \mathcal{B}, \quad (6)$$

where the left hand side term of (6) is the backhaul traffic for BS  $b$  and the right hand side term of (6) is backhaul rate, which must be greater than the backhaul traffic for each BS.  $\zeta_{bn} \in \{0, 1\}$  denotes whether BS  $b$  uses subcarrier  $n$ . For the MFCD scenario,  $\alpha_k$  in (6) is replaced by  $\beta_k^t$  as follows

$$\sum_{k \in \mathcal{K}} \sum_{u \in \mathcal{U}_b} \sum_{m \in \mathcal{M}} s_{bu}^{mt} (1 - \theta_{bk}) \cdot \min \left\{ \sum_{u \in \mathcal{U}_b} v_{ku}, 1 \right\} \beta_k^t \leq \sum_{n \in \mathcal{N}} \zeta_{bn} \tilde{R}_b^{nt}, \forall t \in \mathcal{F}, b \in \mathcal{B}, \quad (7)$$

Note that for all requests of social media  $\omega_k$  from BS  $b$ , if social media  $\omega_k$  is not stored at BS  $b$ , the requested social media  $\omega_k$  is disseminated to BS  $b$  from the core network just once.  $\tilde{R}_b^{nt}$  is the rate of backhaul link for BS  $b$  on subcarrier  $n$  which is calculated by

$$\tilde{R}_b^{nt} = \log_2 (1 + \tilde{\gamma}_b^{nt}), \forall t \in \mathcal{F}, b \in \mathcal{B}, n \in \mathcal{N}. \quad (8)$$

When BS receives the data from core network, it transmits the file back on the downlink. Let  $\tilde{\gamma}_b^{nt}$  denotes the received SNR at BS  $b$  from the core network when the backhaul is used to fetch the files from the core network for BS  $b$ .  $\tilde{\gamma}_b^{nt}$  can be written as  $\tilde{\gamma}_b^{nt} = \frac{\tilde{p}_b^{nt} \tilde{h}_b^{nt}}{(\sigma_b^n)^2}$ , where  $\tilde{p}_b^{nt}$  is the transmit power of each wireless backhaul link connected to BS  $b$  on subcarrier  $n$  and  $\tilde{h}_b^{nt}$  denotes the channel power gains between the  $b^{\text{th}}$  BS on subcarrier  $n$  and the core network and  $(\sigma_b^n)^2$  is the noise power at the  $b^{\text{th}}$  BS on subcarrier  $n$ . Also the downlink traffic should not exceed the capacity of the each downlink capacity which for the first delivery scenario yields

$$\sum_{k \in \mathcal{K}} \sum_{m \in \mathcal{M}} s_{bu}^{mt} v_{ku} \alpha_k \leq \sum_{m \in \mathcal{M}} R_{bu}^{S,mt}, \forall t \in \mathcal{F}, b \in \mathcal{B}, u \in \mathcal{U}_b. \quad (9)$$

Note that for the MFCD scenario,  $\alpha_k$  in (9) is replaced by  $\beta_k^t$  as follows:

$$\sum_{k \in \mathcal{K}} \sum_{m \in \mathcal{M}} s_{bu}^{mt} v_{ku} \beta_k^t \leq \sum_{m \in \mathcal{M}} R_{bu}^{S,mt}, \forall t \in \mathcal{F}, b \in \mathcal{B}, u \in \mathcal{U}_b. \quad (10)$$

*4) Power Allocation Constraints:* To determine the constraints that must be satisfied by any feasible power allocation, let  $p_{bu}^{mt}$  and  $\tilde{p}_b^{nt}$  denote the power allocated to link the  $b^{\text{th}}$  BS-the  $u^{\text{th}}$  user at time slot  $t$  on codebook  $m$  and to link core network-the  $b^{\text{th}}$  BS at frame  $t$ . The elements of  $p_{bu}^{mt}$  and  $\tilde{p}_b^{nt}$  must satisfy the followings:

$$p_{bu}^{mt} \geq 0, \forall b \in \mathcal{B}, u \in \mathcal{U}_b, m \in \mathcal{M}, t \in \mathcal{F}. \quad (11)$$

$$\tilde{p}_b^{nt} \geq 0, \forall b \in \mathcal{B}, n \in \mathcal{N}, t \in \mathcal{F}. \quad (12)$$

In a practical network, core network has a power budget,  $P^{\text{Total},t}$ , which bounds the total power allocated by core network on the core network- $b$  BS links and subcarriers at frame  $t$ . This constraint can be written as

$$\sum_{b \in \mathcal{B}} \sum_{n \in \mathcal{N}} \zeta_{bn} \tilde{p}_b^{nt} \leq P^{\text{Total},t}, \forall t \in \mathcal{F}. \quad (13)$$

5) *EH Constraints*: We assume that the  $b^{\text{th}}$  BS is connected to a rechargeable battery with capacity  $E_b^{\max}$ , and obtains its power supply through an EH renewable solar sources. The solar panels are used to charge batteries during the day.  $E_b^t \in [0, E_b^{\max}]$  is defined as the energy remaining in the battery at the start of the  $t^{\text{th}}$  frame. Then  $E_b^t$  can be written in recursive form as

$$E_b^{t+1} = \min \left( E_b^t - T \sum_{m \in \mathcal{M}} \sum_{u \in \mathcal{U}_b} s_{bu}^{mt} p_{bu}^{mt} + \tilde{E}_b^t, E_b^{\max} \right), \forall b \in \mathcal{B}, t \in \mathcal{F}. \quad (14)$$

where  $\tilde{E}_b^t$  denotes the amount of energy is harvested during the  $t^{\text{th}}$  slot at the  $b^{\text{th}}$  BS. The energy arrival takes place as a Poisson arrival process with mean  $\Gamma$  [32], [33]. The unit amount of energy harvested at each arrival at each BS is denoted by  $\rho$ , which depends on the EH capabilities of renewable energy source at each BS. Therefore,  $\tilde{E}_b^t = \varpi a$ , where  $\varpi$  is the number of arrivals within  $T$  with a mean value of  $\Gamma T$ . In designing of optimal transmission policies for EH communication systems, there are main constraints referred to as energy consumption causality constraints, which state that the energy packets which do not arrive yet, cannot be used by a source. These constraints can be expressed as:

$$\sum_{t=1}^f \sum_{m \in \mathcal{M}} \sum_{u \in \mathcal{U}_b} s_{bu}^{mt} p_{bu}^{mt} \leq \frac{1}{T} \sum_{t=1}^f E_b^t, \forall b \in \mathcal{B}, f \in \mathcal{F}. \quad (15)$$

If battery capacity is not enough to store the newly arrived energy packet, the energy will be wasted at the beginning of a transmission interval. By considering the following constraints on our problem, we avoid this battery overflow by enfrocing the following constraint:

$$\sum_{t=1}^{f+1} E_b^t - T \sum_{t=1}^f \sum_{m \in \mathcal{M}} \sum_{u \in \mathcal{U}_b} s_{bu}^{mt} p_{bu}^{mt} \leq E_b^{\max}, \forall b \in \mathcal{B}, f \in \mathcal{F}. \quad (16)$$

6) *Scheduling Constraints*: It must be guaranteed that each subcarrier cannot be reused more than a certain value  $D$ , i.e., the maximum number of differentiable constellations, as follows:

$$\sum_{b \in \mathcal{B}} \sum_{u \in \mathcal{U}_b} \sum_{m \in \mathcal{M}} c_{nm} s_{bu}^{mt} \leq D, \forall n \in \mathcal{N}, t \in \mathcal{F}. \quad (17)$$

In addition, (18), (19) and (20) together denote that codebooks are exclusively allocated among users of each BS. For the SFCD scenario, we have

$$\sum_{m \in \mathcal{M}} \sum_{t \in \mathcal{F}} \sum_{u \in \mathcal{U}_b} s_{bu}^{mt} \leq 1, \forall b \in \mathcal{B}, \quad (18)$$

and for the MFCD scenario, we have

$$\sum_{m \in \mathcal{M}} \sum_{u \in \mathcal{U}_b} s_{bu}^{mt} \leq 1, \forall b \in \mathcal{B}, t \in \mathcal{F}, \quad (19)$$

$$s_{bu}^{mt} \in \{0, 1\}, \forall b \in \mathcal{B}, u \in \mathcal{U}_b, m \in \mathcal{M}, t \in \mathcal{F}. \quad (20)$$

7) *Worst Case Channel Uncertainty Model*: For the channels between the  $b^{\text{th}}$  BS and the  $q^{\text{th}}$  eavesdropper, only the estimated value  $\tilde{h}_{bq}^{nt}$  is available at the  $b^{\text{th}}$  BS. We define the channel error as  $e_{h_{bq}^{nt}} = h_{bq}^{nt} - \tilde{h}_{bq}^{nt}$ , and we assume that the channels mismatches lie in the bounded sets  $\mathcal{E}_{h_{bq}^{nt}} = \{e_{h_{bq}^{nt}} : e_{h_{bq}^{nt}} \leq \varepsilon_{h_{bq}^{nt}}\}$ , where  $\varepsilon_{h_{bq}^{nt}}$  is known constants.

$$e_{h_{bq}^{nt}} \leq \varepsilon_{h_{bq}^{nt}}, \forall b, q, n, t. \quad (21)$$

### B. The Optimization Problem

We formulate the utility function maximization problem with power allocation, codebook assignment, and content caching subject to energy causality and power budget constraints at each BS for the SFCD scenario as:

$$\begin{aligned} & \max_{\mathbf{p}, \tilde{\mathbf{p}}, \mathbf{s}, \boldsymbol{\theta}, \boldsymbol{\zeta}} \min_{\mathbf{e}_h} \Xi_{\text{EE}}(\mathbf{p}, \mathbf{s}), \\ & \text{s.t. (4), (6), (9), (11) - (18), (20), (21),} \end{aligned} \quad (22)$$

where  $\Xi_{\text{EE}}(\mathbf{p}, \mathbf{s}) = \frac{\sum_{m \in \mathcal{M}} \sum_{t \in \mathcal{F}} \sum_{b \in \mathcal{B}} \sum_{u \in \mathcal{U}_b} R_{bu}^{S,mt}}{\sum_{m \in \mathcal{M}} \sum_{t \in \mathcal{F}} \sum_{b \in \mathcal{B}} \sum_{u \in \mathcal{U}_b} s_{bu}^{mt} p_{bu}^{mt}}$ . Note that for the MFCD scenario, constraint (5) is added to the optimization problem (22). We also replaced (6), (9) and (18) by (7), (10) and (19), respectively. It should also be noted that in the second scenario,  $\boldsymbol{\beta}$  is itself an optimization variable that must be obtained in the optimization problem. (22) is non-convex and includes both integer and continuous variables. Also since this optimization problem is non-convex and NP-hard, it is very difficult to find the global optimal solution within polynomial time. Therefore, the available methods to solve convex optimization problem can not be applied directly. To solve this problem, an iterative algorithm based on the well-known and well-proven alternating, Dinkelbach and successive convex approximation methods is proposed where in each iteration, the main problem is decoupled into several sub-problems subject to some optimization variables.

## IV. PROPOSED SOLUTION

The difficulty of solving the problem (22) arises from the nonconvexity of both the objective function and feasible domain. As far as we know, there is no standard method to solve such a nonconvex optimization problem. In this section, some optimization methods such as alternative optimization, fractional programming, and DC programming, are jointly applied to solve the

primal problem by transforming it into simple subproblems step by step. To facilitate solving (22), an alternate optimization method is adopted to solve a multi-level hierarchical problem which consists of the several subproblem. The core idea of the alternate optimization is that only one of the optimization parameters is optimized in each step while others are fixed. When each parameter is given, the resulting subproblem can be reformulated as the form of DC problem and solved by DC programming. Moreover, a sequential convex program is finally solved by convex optimization methods at each iteration of the DC programming. In this section, we propose solution for the SFCD scenario and note that the MFCD scenario has the same solution. The transformation process for solving this problem mainly consists of the following steps: I. *Transformation of the primal problem*: By using the epigraph method, the inner maximization in the objection function in (25) can be simplified and the secondary problem can be naturally derived. II. *Alternate optimization over some variables*: At this step, the alternate optimization method is adopted to cope with the non-convexity of the resulting parameterized secondary problems which is further rewritten as six sub-problems, namely, access power allocation, access code allocation, backhaul power allocation, backhaul subcarrier allocation, content placement, and channel uncertainty. III. *DC programming for the nonconvex constraint elimination*: At this step, we reformulate the nonconvex constraint (25c) as a canonical DC programming which can be settled by iteratively solving a series of sequential convex constraints. Finally, these convex constraints can be solved by convex programming. IV. *Fractional programming*: By using the fractional programming, the parameterized secondary subproblem is solved with a given parameter at each iteration.

#### A. Transformation of the primal problem

The optimization problem (22) can be further simplified based on the following Lemma 1.

#### **Lemma 1.** The general form of an optimization problem

$$\max_{\mathbf{x}} \{ \Theta_0(\mathbf{x}) - \max_{i \in \Omega} \Theta_i(\mathbf{x}) \} \quad (23a)$$

$$s.t. \quad \mathbf{x} \in \mathbb{X}, \quad (23b)$$

can be transformed into the following form

$$\max_{\mathbf{x}, \tau} \{ \Theta_0(\mathbf{x}) - \tau \} \quad (24a)$$

$$\text{s.t. } \Theta_i(\mathbf{x}) \leq \tau, \forall i \in \Omega, \quad (24b)$$

$$\mathbf{x} \in \mathbb{X}, \quad (24c)$$

by introducing an auxiliary variable  $\tau \in \mathbb{R}$ .

In Lemma 1, the equivalent transformation can be naturally derived by the fact that (24a) is an epigraph of (23a) [34]. It is easily concluded that the optimal  $\tau$  is  $\tau = \max_{i \in \Omega} \Theta_i(\mathbf{x})$  for each fixed  $\mathbf{x}$ . For simplifying (22), we herein introduce auxiliary variables  $\varphi = \{\varphi_{bu}^{mt} \in \mathbb{R}\}$ . Additionally, we can rewrite (22) equivalently as

$$\max_{\mathbf{p}, \tilde{\mathbf{p}}, \mathbf{s}, \boldsymbol{\theta}, \boldsymbol{\zeta}, \boldsymbol{\varphi}} \min_{\mathbf{e}_h} \frac{\sum_{m \in \mathcal{M}} \sum_{t \in \mathcal{F}} \sum_{b \in \mathcal{B}} \sum_{u \in \mathcal{U}_b} \max \left\{ R_{bu}^{D,mt} - \varphi_{bu}^{mt}, 0 \right\}}{\sum_{t \in \mathcal{F}} \sum_{b \in \mathcal{B}} \sum_{m \in \mathcal{M}} \sum_{u \in \mathcal{U}_b} s_{bu}^{mt} p_{bu}^{mt}}, \quad (25a)$$

$$\text{s.t. } \sum_{k \in \mathcal{K}} \sum_{m \in \mathcal{M}} s_{bu}^{mt} v_{ku} \alpha_k \leq \sum_{m \in \mathcal{M}} \max \left\{ R_{bu}^{D,mt} - \varphi_{bu}^{mt}, 0 \right\}, \forall t \in \mathcal{F}, b \in \mathcal{B}, u \in \mathcal{U}_b, \quad (25b)$$

$$R_{buq}^{E,mt} \leq \varphi_{bu}^{mt}, \forall m \in \mathcal{M}, t \in \mathcal{F}, b \in \mathcal{B}, u \in \mathcal{U}_b, q \in \mathcal{Q}, \quad (25c)$$

$$(4), (6), (11), (12), (17) - (21).$$

To solve the optimization problem (25), we should further transform it. We first rewrite  $\max \left\{ R_{bu}^{D,mt} - \varphi_{bu}^{mt}, 0 \right\}$  as [35]:  $\max \left\{ R_{bu}^{D,mt} - \varphi_{bu}^{mt}, 0 \right\} = \max \left\{ -R_{bu2}^{D,mt} - \varphi_{bu}^{mt}, -R_{bu1}^{D,mt} \right\} + R_{bu1}^{D,mt}$  where  $R_{bu1}^{D,mt} = \log_2 \left( \sum_{b \in \mathcal{B}} \sum_{u \in \mathcal{U}_b} \sum_{n \in \mathcal{N}} \left( \eta_{nm} s_{bu}^{mt} p_{bu}^{mt} g_{bu}^{nt} + (\sigma_u^n)^2 \right) \right)$  and  $R_{bu2}^{D,mt} = \log_2 \left( \sum_{b \in \mathcal{B} \setminus \{b\}} \sum_{u \in \mathcal{U}_b} \sum_{n \in \mathcal{N}} \left( \eta_{nm} s_{bu}^{mt} p_{bu}^{mt} g_{bu}^{nt} + (\sigma_u^n)^2 \right) \right)$ . By introducing auxiliary variables  $\boldsymbol{\delta} = \{\delta_{bu}^{mt} \in \mathbb{R}\}$ , (25) is equivalently reformulated as [35]

$$\max_{\mathbf{p}, \tilde{\mathbf{p}}, \mathbf{s}, \boldsymbol{\theta}, \boldsymbol{\zeta}, \boldsymbol{\varphi}, \boldsymbol{\delta}} \min_{\mathbf{e}_h} \left\{ \Theta(\mathbf{p}, \tilde{\mathbf{p}}, \mathbf{s}, \boldsymbol{\theta}, \boldsymbol{\zeta}, \boldsymbol{\varphi}, \mathbf{e}_h) = \frac{\sum_{m \in \mathcal{M}} \sum_{t \in \mathcal{F}} \sum_{b \in \mathcal{B}} \sum_{u \in \mathcal{U}_b} \left\{ \delta_{bu}^{mt} + R_{bu1}^{\mathbf{D},mt} \right\}}{\sum_{t \in \mathcal{F}} \sum_{b \in \mathcal{B}} \sum_{m \in \mathcal{M}} \sum_{u \in \mathcal{U}_b} s_{bu}^{mt} p_{bu}^{mt}} \right\}, \quad (26a)$$

$$\text{s.t. } \sum_{k \in \mathcal{K}} \sum_{m \in \mathcal{M}} s_{bu}^{mt} v_{ku} \alpha_k \leq \sum_{m \in \mathcal{M}} \left\{ \delta_{bu}^{mt} + R_{bu1}^{\mathbf{D},mt} \right\}, \forall t \in \mathcal{F}, b \in \mathcal{B}, u \in \mathcal{U}_b, \quad (26b)$$

$$R_{buq}^{\mathbf{E},mt} \leq \varphi_{bu}^{mt}, \forall m \in \mathcal{M}, t \in \mathcal{F}, b \in \mathcal{B}, u \in \mathcal{U}_b, q \in \mathcal{Q}, \quad (26c)$$

$$- R_{bu2}^{\mathbf{D},mt} - \varphi_{bu}^{mt} \leq \delta_{bu}^{mt}, \forall m \in \mathcal{M}, t \in \mathcal{F}, b \in \mathcal{B}, u \in \mathcal{U}_b, \quad (26d)$$

$$- R_{bu1}^{\mathbf{D},mt} \leq \delta_{bu}^{mt}, \forall m \in \mathcal{M}, t \in \mathcal{F}, b \in \mathcal{B}, u \in \mathcal{U}_b, \quad (26e)$$

(4), (6), (11) – (21).

### B. Alternate optimization over optimization variables

Due to the combined non-convexity of both objective function and the constraint with respect to optimization parameters, the optimization problem (22) is difficult to solve. According to alternate optimization method, we can always optimize a function by first optimizing over some of the variables, and then optimizing over the remaining ones. For convenience, the feasible domain of (22) is denoted by  $\mathbb{D}$  as  $\mathbb{D} \triangleq \{(\mathbf{p}, \tilde{\mathbf{p}}, \mathbf{s}, \boldsymbol{\theta}, \boldsymbol{\zeta}, \mathbf{e}_h) : (4), (6), (9) – (21)\}$ . For the fixed  $\mathbf{p}, \tilde{\mathbf{p}}, \mathbf{s}, \boldsymbol{\theta}, \boldsymbol{\zeta}, \mathbf{e}_h$ -section of the feasible domain of  $\mathbb{D}$ , i.e.,  $\mathbb{D}_{\mathbf{e}_h}$ , is defined as  $\mathbb{D}_{\mathbf{e}_h} \triangleq \{\mathbf{e}_h : (\mathbf{p}, \tilde{\mathbf{p}}, \mathbf{s}, \boldsymbol{\theta}, \boldsymbol{\zeta}, \mathbf{e}_h) \in \mathbb{D}\}$ . Likewise, for the fixed  $\tilde{\mathbf{p}}, \mathbf{s}, \boldsymbol{\theta}, \boldsymbol{\zeta}, \mathbf{e}_h$ ,  $\mathbf{p}$ -section of the feasible domain of  $\mathbb{D}$ , i.e.,  $\mathbb{D}_{\mathbf{p}}$ , is defined as  $\mathbb{D}_{\mathbf{p}} \triangleq \{\mathbf{p} : (\mathbf{p}, \tilde{\mathbf{p}}, \mathbf{s}, \boldsymbol{\theta}, \boldsymbol{\zeta}, \mathbf{e}_h) \in \mathbb{D}\}$ . Similarly, for the fixed  $\mathbf{p}, \tilde{\mathbf{p}}, \boldsymbol{\theta}, \boldsymbol{\zeta}, \mathbf{e}_h$ ,  $\mathbf{s}$ -section of the feasible domain of  $\mathbb{D}$ , i.e.,  $\mathbb{D}_{\mathbf{s}}$ , is defined as  $\mathbb{D}_{\mathbf{s}} \triangleq \{\mathbf{s} : (\mathbf{p}, \tilde{\mathbf{p}}, \mathbf{s}, \boldsymbol{\theta}, \boldsymbol{\zeta}, \mathbf{e}_h) \in \mathbb{D}\}$ . In the same way, for the fixed  $\mathbf{p}, \mathbf{s}, \boldsymbol{\theta}, \boldsymbol{\zeta}, \mathbf{e}_h$ ,  $\tilde{\mathbf{p}}$ -section of the feasible domain of  $\mathbb{D}$ , i.e.,  $\mathbb{D}_{\tilde{\mathbf{p}}}$ , is defined as  $\mathbb{D}_{\tilde{\mathbf{p}}} \triangleq \{\tilde{\mathbf{p}} : (\mathbf{p}, \tilde{\mathbf{p}}, \mathbf{s}, \boldsymbol{\theta}, \boldsymbol{\zeta}, \mathbf{e}_h) \in \mathbb{D}\}$ . Likewise, for the fixed  $\mathbf{p}, \tilde{\mathbf{p}}, \mathbf{s}, \boldsymbol{\theta}, \mathbf{e}_h$ ,  $\boldsymbol{\zeta}$ -section of the feasible domain of  $\mathbb{D}$ , i.e.,  $\mathbb{D}_{\boldsymbol{\zeta}}$ , is defined as  $\mathbb{D}_{\boldsymbol{\zeta}} \triangleq \{\boldsymbol{\zeta} : (\mathbf{p}, \tilde{\mathbf{p}}, \mathbf{s}, \boldsymbol{\theta}, \boldsymbol{\zeta}, \mathbf{e}_h) \in \mathbb{D}\}$ . Correspondingly, for the fixed  $\tilde{\mathbf{p}}, \mathbf{s}, \boldsymbol{\theta}, \boldsymbol{\zeta}, \mathbf{e}_h$ ,  $\boldsymbol{\theta}$ -section of the feasible domain of  $\mathbb{D}$ , i.e.,  $\mathbb{D}_{\boldsymbol{\theta}}$ , is defined as  $\mathbb{D}_{\boldsymbol{\theta}} \triangleq \{\boldsymbol{\theta} : (\mathbf{p}, \tilde{\mathbf{p}}, \mathbf{s}, \boldsymbol{\theta}, \boldsymbol{\zeta}, \mathbf{e}_h) \in \mathbb{D}\}$ . Finally, the alternate optimization is used to solve the following hierarchical six-level optimization subproblem:

$$\max_{\mathbf{p} \in \mathbb{D}_{\mathbf{p}}, \boldsymbol{\varphi} \in \mathbb{R}, \boldsymbol{\delta} \in \mathbb{R}} \left\{ \max_{\mathbf{s} \in \mathbb{D}_{\mathbf{s}}} \left\{ \max_{\tilde{\mathbf{p}} \in \mathbb{D}_{\tilde{\mathbf{p}}}} \left\{ \max_{\boldsymbol{\zeta} \in \mathbb{D}_{\boldsymbol{\zeta}}} \left\{ \max_{\boldsymbol{\theta} \in \mathbb{D}_{\boldsymbol{\theta}}} \left\{ \min_{\mathbf{e}_h \in \mathbb{D}_{\mathbf{e}_h}} \Theta(\mathbf{p}, \tilde{\mathbf{p}}, \mathbf{s}, \boldsymbol{\theta}, \boldsymbol{\zeta}, \boldsymbol{\varphi}, \mathbf{e}_h) \right\} \right\} \right\} \right\} \right\}. \quad (27)$$

In conclusion, the subproblems can be solved sequentially at each iteration of alternate optimization. In the first optimization subproblem, we find  $\mathbf{e}_h$  for a given  $\mathbf{p}_{\varrho}, \mathbf{s}_{\varrho}, \boldsymbol{\varphi}_{\varrho}$ , and  $\boldsymbol{\delta}_{\varrho}$

$$\min_{\mathbf{e}_h \in \mathbb{D}_{\mathbf{e}_h}} \Theta(\mathbf{p}_{\varrho}, \tilde{\mathbf{p}}_{\varrho}, \mathbf{s}_{\varrho}, \boldsymbol{\theta}_{\varrho}, \boldsymbol{\zeta}_{\varrho}, \boldsymbol{\varphi}_{\varrho}, \mathbf{e}_{h\varrho}), \quad (28)$$

where  $\varrho$  is the iteration number of alternate optimization algorithm. By defining the solution of (28) as  $\mathbf{e}_{h\varrho+1}$ , the second level subproblem is solved to find  $\boldsymbol{\theta}$  with a given  $\mathbf{p}_\varrho, \mathbf{s}_\varrho, \boldsymbol{\varphi}_\varrho$ , and  $\boldsymbol{\delta}_\varrho$

$$\max_{\boldsymbol{\theta} \in \mathbb{D}_{\boldsymbol{\theta}}} \Theta(\mathbf{p}_\varrho, \tilde{\mathbf{p}}_\varrho, \mathbf{s}_\varrho, \boldsymbol{\theta}_\varrho, \boldsymbol{\zeta}_\varrho, \boldsymbol{\varphi}_\varrho, \mathbf{e}_{h\varrho}). \quad (29)$$

Similarly, by defining the solution of (29) as  $\boldsymbol{\theta}_{\varrho+1}$ , the third level subproblem is solved to find  $\boldsymbol{\zeta}$  with a given  $\mathbf{p}_\varrho, \mathbf{s}_\varrho, \boldsymbol{\varphi}_\varrho$ , and  $\boldsymbol{\delta}_\varrho$

$$\max_{\boldsymbol{\zeta} \in \mathbb{D}_{\boldsymbol{\zeta}}} \Theta(\mathbf{p}_\varrho, \tilde{\mathbf{p}}_\varrho, \mathbf{s}_\varrho, \boldsymbol{\theta}_\varrho, \boldsymbol{\zeta}_\varrho, \boldsymbol{\varphi}_\varrho, \mathbf{e}_{h\varrho}). \quad (30)$$

In a similar manner, by defining the solution of (30) as  $\boldsymbol{\zeta}_{\varrho+1}$ , the fourth level subproblem is solved to find  $\tilde{\mathbf{p}}$  with a given  $\mathbf{p}_\varrho, \mathbf{s}_\varrho, \boldsymbol{\varphi}_\varrho$ , and  $\boldsymbol{\delta}_\varrho$

$$\max_{\tilde{\mathbf{p}} \in \mathbb{D}_{\tilde{\mathbf{p}}}} \Theta(\mathbf{p}_\varrho, \tilde{\mathbf{p}}_\varrho, \mathbf{s}_\varrho, \boldsymbol{\theta}_\varrho, \boldsymbol{\zeta}_\varrho, \boldsymbol{\varphi}_\varrho, \mathbf{e}_{h\varrho}). \quad (31)$$

Correspondingly, by defining the solution of (31) as  $\tilde{\mathbf{p}}_{\varrho+1}$ , the fifth level subproblem is solved to find  $\mathbf{s}$  with a given  $\mathbf{p}_\varrho, \boldsymbol{\varphi}_\varrho$ , and  $\boldsymbol{\delta}_\varrho$

$$\max_{\mathbf{s} \in \mathbb{D}_{\mathbf{s}}} \Theta(\mathbf{p}_\varrho, \tilde{\mathbf{p}}_\varrho, \mathbf{s}_\varrho, \boldsymbol{\theta}_\varrho, \boldsymbol{\zeta}_\varrho, \boldsymbol{\varphi}_\varrho, \mathbf{e}_{h\varrho}). \quad (32)$$

Finally, by defining the solution of (32) as  $\mathbf{s}_{\varrho+1}$ , the sixth level subproblem is solved to find  $\mathbf{p}, \boldsymbol{\varphi}, \boldsymbol{\delta}$  with a given  $\mathbf{s}_\varrho$

$$\max_{\mathbf{p} \in \mathbb{D}_{\mathbf{p}}, \boldsymbol{\varphi}, \boldsymbol{\delta}} \Theta(\mathbf{p}_\varrho, \tilde{\mathbf{p}}_\varrho, \mathbf{s}_\varrho, \boldsymbol{\theta}_\varrho, \boldsymbol{\zeta}_\varrho, \boldsymbol{\varphi}_\varrho, \mathbf{e}_{h\varrho}). \quad (33)$$

Let  $(\mathbf{p}_\varrho, \tilde{\mathbf{p}}_\varrho, \mathbf{s}_\varrho, \boldsymbol{\theta}_\varrho, \boldsymbol{\zeta}_\varrho, \mathbf{e}_{h\varrho})$  denote the obtained solution at the  $\varrho$ -th iteration, which should be used for the  $\varrho + 1$ -th iteration. With a convergence threshold  $\epsilon_1$ , the stop condition of alternate optimization algorithm is then given by

$$|\Theta(\mathbf{p}_\varrho, \tilde{\mathbf{p}}_\varrho, \mathbf{s}_\varrho, \boldsymbol{\theta}_\varrho, \boldsymbol{\zeta}_\varrho, \boldsymbol{\varphi}_\varrho, \mathbf{e}_{h\varrho}) - \Theta(\mathbf{p}_{\varrho+1}, \tilde{\mathbf{p}}_{\varrho+1}, \mathbf{s}_{\varrho+1}, \boldsymbol{\theta}_{\varrho+1}, \boldsymbol{\zeta}_{\varrho+1}, \boldsymbol{\varphi}_{\varrho+1}, \mathbf{e}_{h\varrho+1})| \leq \epsilon_1. \quad (34)$$

We can also present a maximum allowed number  $\Psi_1$  for  $\varrho_1$ . Alternate optimization algorithm is illustrated in Table. I. Furthermore, the following Theorem. 1 can verify the convergence of the alternate optimization algorithm.

**Theorem 1.** *If (28) -(33) are solvable, in each iteration, the sequence of each solution, i.e.,  $\{\Theta(\mathbf{p}_\varrho, \mathbf{s}_\varrho, \boldsymbol{\varphi}_\varrho, \boldsymbol{\delta}_\varrho)\}$ , is monotonically decreasing.* □

*Proof.* Please see Appindex A. □

TABLE I  
ALTERNATE OPTIMIZATION ALGORITHM

**Algorithm 1:** Alternate Optimization Algorithm

---

**Step1:** Select a starting point  $(\mathbf{p}_0, \tilde{\mathbf{p}}_0, \mathbf{s}_0, \boldsymbol{\theta}_0, \boldsymbol{\zeta}_0, \boldsymbol{\varphi}_0, \boldsymbol{\delta}_0) \in \mathbb{D}$ , and Set iteration number  $\varrho = 0$ ;

**Step2:** Compute  $\Theta(\mathbf{p}_0, \mathbf{s}_0, \boldsymbol{\varphi}_0, \boldsymbol{\delta}_0)$ ;

**Repeat**

**Step3:** For the fixed  $\mathbf{p}_\varrho$ , solve (35) to obtained the  $\mathbf{e}_{h_{\varrho+1}}$  (Semidefinite programming (SDP));

**Step4:** For the obtained  $\mathbf{e}_{h_{\varrho+1}}$ , and fixed  $\mathbf{p}_\varrho, \tilde{\mathbf{p}}_\varrho, \mathbf{s}_\varrho, \boldsymbol{\zeta}_\varrho, \boldsymbol{\varphi}_\varrho, \boldsymbol{\delta}_\varrho$ , solve (29) to find  $\boldsymbol{\theta}_{\varrho+1}$  (Linear programming);

**Step5:** For the obtained  $\mathbf{e}_{h_{\varrho+1}}$  and  $\boldsymbol{\theta}_{\varrho+1}$ , and fixed  $\mathbf{p}_\varrho, \tilde{\mathbf{p}}_\varrho, \mathbf{s}_\varrho, \boldsymbol{\varphi}_\varrho, \boldsymbol{\delta}_\varrho$ , solve (30) to find  $\boldsymbol{\zeta}_{\varrho+1}$  (Convex programming);

**Step6:** For the obtained  $\mathbf{e}_{h_{\varrho+1}}, \boldsymbol{\theta}_{\varrho+1}$  and  $\boldsymbol{\zeta}_{\varrho+1}$ , and fixed  $\mathbf{p}_\varrho, \mathbf{s}_\varrho, \boldsymbol{\varphi}_\varrho, \boldsymbol{\delta}_\varrho$ , solve (31) to find  $\tilde{\mathbf{p}}_{\varrho+1}$  (Convex programming);

**Step7:** For the obtained  $\mathbf{e}_{h_{\varrho+1}}, \boldsymbol{\theta}_{\varrho+1}, \boldsymbol{\zeta}_{\varrho+1}$  and  $\tilde{\mathbf{p}}_{\varrho+1}$ , and fixed  $\mathbf{p}_\varrho, \boldsymbol{\varphi}_\varrho, \boldsymbol{\delta}_\varrho$ , solve (32) to find  $\mathbf{s}_{\varrho+1}$  (DC programming);

**Step8:** For the obtained  $\mathbf{e}_{h_{\varrho+1}}, \boldsymbol{\theta}_{\varrho+1}, \boldsymbol{\zeta}_{\varrho+1}, \tilde{\mathbf{p}}_{\varrho+1}$  and  $\mathbf{s}_{\varrho+1}$ , solve (33) to find  $\mathbf{p}_{\varrho+1}, \boldsymbol{\varphi}_{\varrho+1}$  and  $\boldsymbol{\delta}_{\varrho+1}$  (DC programming);

**Step9:** Compute  $\Theta(\mathbf{p}_{\varrho+1}, \mathbf{s}_{\varrho+1}, \boldsymbol{\varphi}_{\varrho+1}, \boldsymbol{\delta}_{\varrho+1})$ ;

**Step10:**  $\varrho = \varrho + 1$ ;

**Step11:** **If**  $|\Theta(\mathbf{p}_\varrho, \mathbf{s}_\varrho, \boldsymbol{\varphi}_\varrho, \boldsymbol{\delta}_\varrho) - \Theta(\mathbf{p}_{\varrho+1}, \mathbf{s}_{\varrho+1}, \boldsymbol{\varphi}_{\varrho+1}, \boldsymbol{\delta}_{\varrho+1})| \leq \epsilon_1$  or  $\varrho > \Psi_1$  goto Step12, **else** goto Step3;

**End**

**Step12:** Return  $(\mathbf{p}, \tilde{\mathbf{p}}, \mathbf{s}, \boldsymbol{\theta}, \boldsymbol{\zeta}, \boldsymbol{\varphi}, \boldsymbol{\delta}) = (\mathbf{p}_\varrho, \tilde{\mathbf{p}}_\varrho, \mathbf{s}_\varrho, \boldsymbol{\theta}_\varrho, \boldsymbol{\zeta}_\varrho, \boldsymbol{\varphi}_\varrho, \boldsymbol{\delta}_\varrho)$ .

---

1) *Channel Uncertainty Problem:* Minimizing the worst-case problem over  $e_{h_{bq}^{nt}}$  in (28) is equivalent to the following problem:

$$\min_{e_{h_{bq}^{nt}}} p_{bu}^{mt} (\tilde{h}_{bq}^{nt} + e_{h_{bq}^{nt}}) (\tilde{h}_{bq}^{nt} + e_{h_{bq}^{nt}})^\dagger, \quad \text{s.t. (21).} \quad (35)$$

This problem is convex since its Hessian is positive semidefinite, and thus strong duality holds for (35) and its dual. The worst-case channel mismatch is provided through the following proposition.

**Proposition 1.** *The worst channel mismatch for problem (35) is given by  $e_{h_{bq}^{nt}}^* = -\tilde{h}_{bq}^{nt} p_{bu}^{mt} (\lambda_{bq}^{nt} + p_{bu}^{mt})$ , which is the solution of the following SDP problem*

$$\max_{\lambda_{bq}^{nt} \geq 0, \varpi_{bq}^{nt}} \varpi_{bq}^{nt} \quad (36a)$$

$$S.t : \begin{bmatrix} \lambda_{bq}^{nt} + p_{bu}^{mt} & p_{bu}^{mt} \tilde{h}_{bq}^{nt} \\ p_{bu}^{mt} \tilde{h}_{bq}^{nt} & p_{bu}^{mt} \tilde{h}_{bq}^{nt} \tilde{h}_{bq}^{nt\dagger} - \lambda_{bq}^{nt} \varepsilon_{h_{bq}^{nt}} - \varpi_{bq}^{nt} \end{bmatrix}. \quad (36b)$$

2) *Content Placement*: A linear programming (LP) with respect to  $\boldsymbol{\theta}$  for the content placement problem can be obtained. This problem can be easily solved by existing LP available standard optimization softwares such as CVX with the internal solver MOSEK [13], [36].

3) *Backhaul Power and Subcarrier Allocation*: The optimization problem is still a mixed-integer non-convex programming with respect to  $\zeta$  and  $\tilde{\mathbf{p}}$ , which is difficult to tackle. To make this problem tractable, we first relax each  $\zeta$  to a continuous interval, i.e.,  $\zeta \in [0,1]$ . Further, the new variables  $\mathbf{x} = \zeta \tilde{\mathbf{p}}$  is defined to replace  $\tilde{\mathbf{p}}$ . This problem can be easily solved by available standard optimization softwares such as CVX with the internal solver MOSEK [13].

4) *Access Power and Codebook Allocation*: The optimization problem is still non-convex with respect to  $\mathbf{p}$  and  $\mathbf{s}$ . The difficulty of solution comes from the non-convexity of both objective function and secrecy rate constraint. There is no standard approach to solve such a non-convex problem. Therefore, we exploit DC and fractional programming in the next sections to transform into a tractable problem.

### C. Difference-of-Two-Concave-Functions (D.C.) Approximation

Due to the non-convexity of (26c), the optimization problem (26) is still difficult to solve. The standard D.C. optimization problem can be written as  $\min_{\mathbf{x}} \{F(\mathbf{x}) = F_1(\mathbf{x}) - F_2(\mathbf{x})\}$  where  $F_1$  and  $F_2$  are two convex components with convex feasible domain. This problem can be solved iteratively by solving a sequential convex program as follows:

$$\min_{\mathbf{x}} \{F_1(\mathbf{x}) - F_2(\mathbf{x}_\varrho) - \langle \nabla F_2(\mathbf{x}_\varrho), \mathbf{x} - \mathbf{x}_\varrho \rangle\}, \quad (37)$$

at each iteration, where  $\mathbf{x}_\varrho$  is the optimal solution of the  $\varrho^{\text{th}}$  iteration used for the  $(\varrho+1)^{\text{th}}$  iteration and  $\nabla F_2(\mathbf{x})$  is the gradient of  $F_2(\mathbf{x})$  evaluated at  $\mathbf{x}_\varrho$ . By the D.C. programming approximation, DC subproblems are equivalently reformulated as

$$\max_{\mathbf{p}, \boldsymbol{\varphi}, \boldsymbol{\delta}} \Theta(\mathbf{p}_\varrho, \tilde{\mathbf{p}}_\varrho, \mathbf{s}_\varrho, \boldsymbol{\theta}_\varrho, \zeta_\varrho, \boldsymbol{\varphi}_\varrho, \mathbf{e}_{h\varrho}), \quad (38a)$$

$$\text{s.t. } - \left( R_{buq2}^{\text{E},mt} - R_{buq1}^{\text{E},mt} - \left\langle \nabla R_{bu1}^{\text{E},t}, p_{bu}^{mt} - p_{bu}^{mt}(\varrho) \right\rangle \right) \leq \varphi_{bu}^{mt}, \forall m \in \mathcal{M}, t \in \mathcal{F}, b \in \mathcal{B}, u \in \mathcal{U}_b, q \in \mathcal{Q}, \quad (38b)$$

(11), (15), (16), (26b), (26d), (26e),

where  $R_{buq1}^{E,mt} = \log_2 \left( \sum_{b \in \mathcal{B}} \sum_{u \in \mathcal{U}_b} \sum_{n \in \mathcal{N}} \left( \eta_{nm} s_{bu}^{mt} p_{bu}^{mt} h_{bq}^{nt} + (\sigma_q^n)^2 \right) \right)$  and  $R_{bu2}^{E,mt} = \log_2 \left( \sum_{b \in \mathcal{B} \setminus \{b\}} \sum_{u \in \mathcal{U}_b} \sum_{n \in \mathcal{N}} \left( \eta_{nm} s_{bu}^{mt} p_{bu}^{mt} h_{bq}^{nt} + (\sigma_q^n)^2 \right) \right)$  and

$$\max_{\mathbf{s}} \Theta(\mathbf{p}_\varrho, \tilde{\mathbf{p}}_\varrho, \mathbf{s}_\varrho, \boldsymbol{\theta}_\varrho, \boldsymbol{\zeta}_\varrho, \boldsymbol{\varphi}_\varrho, \mathbf{e}_{h\varrho}), \quad (39a)$$

$$\text{s.t. } - \left( R_{buq2}^{E,mt} - R_{buq1}^{E,mt} - \left\langle \nabla R_{bu1}^{E,t}, s_{bu}^{mt} - s_{bu}^{mt}(\varrho) \right\rangle \right) \leq \varphi_{bu}^{mt}, \forall m \in \mathcal{M}, t \in \mathcal{F}, b \in \mathcal{B}, u \in \mathcal{U}_b, q \in \mathcal{Q}, \quad (39b)$$

(6), (15), (16), (17), (18), (20), (26b), (26d), (26e).

We first express  $R_{buq}^{E,mt}$  in a D.C. form as

$$R_{buq}^{E,mt} = -(R_{buq2}^{E,mt} - R_{buq1}^{E,mt}), \quad (40)$$

Based on (40), the gradient  $\nabla R_{bu1}^{E,mt}$  with respect to  $\mathbf{p}$  is given by

$$\nabla R_{bu1}^{E,mt} = \frac{\partial R_{bu1}^{E,mt}}{\partial p_{bu}^{mt}} = \frac{\partial R_{buq1}^{E,mt}}{\partial p_{bu}^{mt}} = \frac{s_{bu}^{mt}}{\ln 2} \frac{\sum_{n \in \mathcal{N}} (\eta_{nm} h_{bq}^{nt})}{\sum_{b \in \mathcal{B}} \sum_{u \in \mathcal{U}_b} \sum_{n \in \mathcal{N}} (\eta_{nm} s_{bu}^{mt} p_{bu}^{mt} h_{bq}^{nt} + (\sigma_q^n)^2)}, \quad (41)$$

Similarly, the gradient  $\nabla R_{bu1}^{E,mt}$  with respect to  $\mathbf{s}$  is given by

$$\nabla R_{buq1}^{E,mt} = \frac{\partial R_{buq1}^{E,mt}}{\partial s_{bu}^{mt}} = \frac{\partial R_{bu1}^{E,mt}}{\partial s_{bu}^{mt}} = \frac{p_{bu}^{mt}}{\ln 2} \frac{\sum_{n \in \mathcal{N}} (\eta_{nm} h_{bq}^{nt})}{\sum_{b \in \mathcal{B}} \sum_{u \in \mathcal{U}_b} \sum_{n \in \mathcal{N}} (\eta_{nm} s_{bu}^{mt} p_{bu}^{mt} h_{bq}^{nt} + (\sigma_q^n)^2)}, \quad (42)$$

**Theorem 2.** *The sequence  $R_{buq}^{E,mt}$  derived from the D.C. programming algorithm is monotonously decreasing.*  $\square$

*Proof.* Please see Appendix B.  $\square$

The DC programming is expounded in Algorithm 1, where  $\varrho$ ,  $\zeta$ , and  $I_\zeta$  represent the iterative index, the convergence threshold, and the maximum allowed number of  $\varrho$ , respectively. D.C. programming algorithm is shown in Table. II

#### D. Fractional Programming

The objective function in (26) is non-convex. The form of (26) can be classed into the nonlinear fractional programming [37]. Therefore, after replacing nonconvex constraints by convex constraints using the D.C. method in the previous section, the Dinkelbach's algorithm use to solve convex fractional programming. We define the maximum objective function  $\chi^*$  of the considered system as:

$$\chi^* = \max_{\mathbf{p}, \mathbf{s}, \boldsymbol{\varphi}, \boldsymbol{\delta}} \frac{\sum_{m \in \mathcal{M}} \sum_{t \in \mathcal{F}} \sum_{b \in \mathcal{B}} \sum_{u \in \mathcal{U}_b} \left\{ \delta_{bu}^{mt} + R_{bu1}^{D,mt} \right\}}{\sum_{t \in \mathcal{F}} \sum_{b \in \mathcal{B}} \sum_{m \in \mathcal{M}} \sum_{u \in \mathcal{U}_b} s_{bu}^{mt} p_{bu}^{mt}} = \frac{\Xi_{\text{Num}}(\mathbf{p}, \mathbf{s}, \boldsymbol{\varphi}, \boldsymbol{\delta})}{\Xi_{\text{Den}}(\mathbf{p}, \mathbf{s}, \boldsymbol{\varphi}, \boldsymbol{\delta})} \quad (43)$$

TABLE II  
DC PROGRAMMING ALGORITHM

**Algorithm 2:** DC Programming Algorithm

---

**Step1:** Initialize the value  $\mathbf{p}_0, \mathbf{s}_0, \boldsymbol{\varphi}_0, \boldsymbol{\delta}_0$  and iteration number set  $\varrho = 0$ ;

**Step2:** Compute  $\Theta(\mathbf{p}_\varrho, \mathbf{s}_\varrho, \boldsymbol{\varphi}_\varrho, \boldsymbol{\delta}_\varrho)$ ;

**Repeat**

**Step3:** For  $\mathbf{s}_\varrho$  solve the problem in (38) to obtain  $\mathbf{p}_{\varrho+1}, \boldsymbol{\varphi}_{\varrho+1}, \boldsymbol{\delta}_{\varrho+1}$  by Fractional programming;

**Step4:** For  $\mathbf{p}_{\varrho+1}, \boldsymbol{\varphi}_{\varrho+1}, \boldsymbol{\delta}_{\varrho+1}$  solve the problem in (39) to obtain  $\mathbf{s}_{\varrho+1}$  by Fractional programming;

**Step5:** Compute  $\Theta(\mathbf{p}_{\varrho+1}, \mathbf{s}_{\varrho+1}, \boldsymbol{\varphi}_{\varrho+1}, \boldsymbol{\delta}_{\varrho+1})$ ;

**Step6:**  $\varrho = \varrho + 1$ ;

**Step7:** **If**  $|\Theta(\mathbf{p}_\varrho, \mathbf{s}_\varrho, \boldsymbol{\varphi}_\varrho, \boldsymbol{\delta}_\varrho) - \Theta(\mathbf{p}_{\varrho+1}, \mathbf{s}_{\varrho+1}, \boldsymbol{\varphi}_{\varrho+1}, \boldsymbol{\delta}_{\varrho+1})| \leq \epsilon_2$  or  $\varrho > \Psi_2$  goto Step8, **else** goto Step3;

**End**

**Step8:** Return  $(\mathbf{p}, \tilde{\mathbf{p}}, \mathbf{s}, \boldsymbol{\theta}, \boldsymbol{\zeta}, \boldsymbol{\varphi}, \boldsymbol{\delta}) = (\mathbf{p}_\varrho, \tilde{\mathbf{p}}_\varrho, \mathbf{s}_\varrho, \boldsymbol{\theta}_\varrho, \boldsymbol{\zeta}_\varrho, \boldsymbol{\varphi}_\varrho, \boldsymbol{\delta}_\varrho)$ .

---

We are now ready to introduce the following theorem.

**Theorem 3.** *The maximum value of  $\chi^*$  is achieved if and only if*

$$\begin{aligned} \max_{\mathbf{p}, \mathbf{s}, \boldsymbol{\varphi}, \boldsymbol{\delta}} \quad & \{\Xi_{Num}(\mathbf{p}, \mathbf{s}, \boldsymbol{\varphi}, \boldsymbol{\delta}) - \chi^* \Xi_{Dem}(\mathbf{p}, \mathbf{s}, \boldsymbol{\varphi}, \boldsymbol{\delta})\} \\ & = \Xi_{Num}(\mathbf{p}^*, \mathbf{s}^*, \boldsymbol{\varphi}^*, \boldsymbol{\delta}^*) - \chi^* \Xi_{Num}(\mathbf{p}^*, \mathbf{s}^*, \boldsymbol{\varphi}^*, \boldsymbol{\delta}^*) = 0, \end{aligned} \quad (44)$$

For  $\Xi_{Num}(\mathbf{p}, \mathbf{s}, \boldsymbol{\varphi}, \boldsymbol{\delta}) \geq 0$  and  $\Xi_{Dem}(\mathbf{p}, \mathbf{s}, \boldsymbol{\varphi}, \boldsymbol{\delta}) > 0$ , where

$$\max_{\mathbf{p}, \mathbf{s}, \boldsymbol{\varphi}, \boldsymbol{\delta}} \quad \{\Xi_{Num}(\mathbf{p}, \mathbf{s}, \boldsymbol{\varphi}, \boldsymbol{\delta}) - \chi \Xi_{Dem}(\mathbf{p}, \mathbf{s}, \boldsymbol{\varphi}, \boldsymbol{\delta})\}, \quad (45)$$

is defined as a parametric program with parameter  $\chi$ . □

*Proof.* Please refer to [37], [38]. □

By the Dinkelbach's method [23] with a initial value  $\chi_0$  of  $\chi$ , (45) can be solved iteratively by solving

$$\max_{\mathbf{p}, \mathbf{s}, \boldsymbol{\varphi}, \boldsymbol{\delta}} \Xi_{Num}(\mathbf{p}, \mathbf{s}, \boldsymbol{\varphi}, \boldsymbol{\delta}) - \chi_\varrho \Xi_{Dem}(\mathbf{p}, \mathbf{s}, \boldsymbol{\varphi}, \boldsymbol{\delta}), \quad (46)$$

with a given  $\chi_\varrho$  at the  $\varrho^{\text{th}}$  iteration, where  $\varrho$  is the iteration index.  $\chi_\varrho$  can be explained as the secure EE obtained at the previous iteration. In (46), the maximization problem is equivalent to

$$\min_{\mathbf{p}, \mathbf{s}, \boldsymbol{\varphi}, \boldsymbol{\delta}} \chi_\varrho \Xi_{Dem}(\mathbf{p}, \mathbf{s}, \boldsymbol{\varphi}, \boldsymbol{\delta}) - \Xi_{Num}(\mathbf{p}, \mathbf{s}, \boldsymbol{\varphi}, \boldsymbol{\delta}), \quad (47)$$

in the sense of the same solution set. Let  $\mathbf{p}(\chi_\varrho), \boldsymbol{\varphi}(\chi_\varrho)$  and  $\boldsymbol{\delta}(\chi_\varrho)$  denote the solution of (48) for a given  $\chi_\varrho$ . After each iteration,  $\chi_\varrho$  should be updated by

$$\chi_{\varrho+1} = \frac{\Xi_{\text{Dem}}(\mathbf{p}(\chi_\varrho), \boldsymbol{\varphi}(\chi_\varrho), \boldsymbol{\delta}(\chi_\varrho), \mathbf{s})}{\Xi_{\text{Num}}(\mathbf{p}(\chi_\varrho), \boldsymbol{\varphi}(\chi_\varrho), \boldsymbol{\delta}(\chi_\varrho), \mathbf{s})}. \quad (48)$$

The iteration process will be stopped when (44) is satisfied. In practice, we define the terminated condition of the iterative process as

$$|\chi_\varrho \Xi_{\text{Dem}}(\mathbf{p}(\chi_\varrho), \boldsymbol{\varphi}(\chi_\varrho), \boldsymbol{\delta}(\chi_\varrho), \mathbf{s}) - \Xi_{\text{Num}}(\mathbf{p}(\chi_\varrho), \boldsymbol{\varphi}(\chi_\varrho), \boldsymbol{\delta}(\chi_\varrho), \mathbf{s})| \leq \epsilon_3, \quad (49)$$

with a small convergence tolerance  $\epsilon_3 > 0$ . The algorithm of fractional programming is clarified in Algorithm 2, where  $\Psi_3$  is the maximum allowed number of iterations considering the computational time. We use the fractional programming dincklebuch's algorithm for the convexified problem (38) and (39).

**Theorem 4.** *If problems (50) and (51) are solvable, the sequence  $\{\chi_\varrho\}$  obtained by Algorithm 1 has the following properties: 1)  $\chi_{\varrho+1} > \chi_\varrho$ ; 2)  $\lim_{\varrho \rightarrow \infty} \chi_\varrho = \chi^*$ .*  $\square$

*Proof.* Please refer to [37].  $\square$

Based on the fractional programming, fractional subproblems (50) and (51) are associated with a parametric program problem stated as follows:

$$\max_{\mathbf{p}, \boldsymbol{\varphi}, \boldsymbol{\delta}} \chi \sum_{t \in \mathcal{F}} \sum_{b \in \mathcal{B}} \sum_{m \in \mathcal{M}} \sum_{u \in \mathcal{U}_b} s_{bu}^{mt} p_{bu}^{mt} - \sum_{m \in \mathcal{M}} \sum_{t \in \mathcal{F}} \sum_{b \in \mathcal{B}} \sum_{u \in \mathcal{U}_b} \left\{ \delta_{bu}^{mt} + R_{bu1}^{\text{D},mt} \right\}, \quad (50a)$$

$$\text{s.t. } - \left( R_{buq2}^{\text{E},mt} - R_{buq1}^{\text{E},mt} - \left\langle \nabla R_{bu1}^{\text{E},t}, p_{bu}^{mt} - p_{bu}^{mt}(\varrho) \right\rangle \right) \leq \varphi_{bu}^{mt}, \forall m \in \mathcal{M}, t \in \mathcal{F}, b \in \mathcal{B}, u \in \mathcal{U}_b, q \in \mathcal{Q}, \quad (50b)$$

(11), (15), (16), (26b), (26d), (26e).

and

$$\max_{\mathbf{s}} \chi \sum_{t \in \mathcal{F}} \sum_{b \in \mathcal{B}} \sum_{m \in \mathcal{M}} \sum_{u \in \mathcal{U}_b} s_{bu}^{mt} p_{bu}^{mt} - \sum_{m \in \mathcal{M}} \sum_{t \in \mathcal{F}} \sum_{b \in \mathcal{B}} \sum_{u \in \mathcal{U}_b} \left\{ \delta_{bu}^{mt} + R_{bu1}^{\text{D},mt} \right\}, \quad (51a)$$

$$\text{s.t. } - \left( R_{buq2}^{\text{E},mt} - R_{buq1}^{\text{E},mt} - \left\langle \nabla R_{bu1}^{\text{E},t}, s_{bu}^{mt} - s_{bu}^{mt}(\varrho) \right\rangle \right) \leq \varphi_{bu}^{mt}, \forall m \in \mathcal{M}, t \in \mathcal{F}, b \in \mathcal{B}, u \in \mathcal{U}_b, q \in \mathcal{Q}, \quad (51b)$$

(6), (15) – (20), (26b), (26d), (26e).

We propose an iterative algorithm (known as the Dinkelbach method [37]) for solving (50) and (51) with an equivalent objective function. The proposed algorithm is summarized in Table. III and the convergence to the optimal energy efficiency is guaranteed.

TABLE III  
FRACTIONAL PROGRAMMING ALGORITHM

---

**Algorithm 3:** Fractional Programming Algorithm

---

**Step1:** Initialize the maximum number of iterations  $\Psi_3$  and the maximum tolerance  $\epsilon_3$ ;  
**Step2:** Choose an initial value  $\chi_0$  and set iteration index  $\varrho = 0$ ;  
**Repeat**  
**Step3:** Solve problem (50) for a given  $\chi_\varrho$  and obtain power allocation policy  $\mathbf{p}(\chi_\varrho)$  (Convex programming);  
**Step4:** Solve problem (51) for a given  $\chi_\varrho$  and obtain code assignment policy  $\mathbf{s}(\chi_\varrho)$  (Convex programming);  
**Step5:** Update  $\chi_\varrho$  by (48) to obtain  $\chi_{\varrho+1}$ ;  
**Step6:**  $\varrho = \varrho + 1$ ;  
**Step7:** If  $|\chi_\varrho \Xi_{\text{Den}}(\mathbf{p}(\chi_\varrho), \mathbf{s}(\chi_\varrho)) - \Xi_{\text{Num}}(\mathbf{p}(\chi_\varrho), \mathbf{s}(\chi_\varrho))| < \epsilon_3$  or  $\varrho > \Psi_3$  goto Step7, **else** goto Step3;  
**Step8:** Return  $\mathbf{p}^* = \mathbf{p}(\chi_{\varrho-1})$ ,  $\mathbf{s}^* = \mathbf{s}(\chi_{\varrho-1})$  and  $\chi^* = \chi_\varrho$ .  
**End**

---

## V. ANALYSIS OF COMPUTATIONAL COMPLEXITY OF PROPOSED ALGORITHM

To solve the primary optimization problem, the main optimization problem is decomposed into several subproblems, with each subproblem being in a hierarchical order of the main problem. The fast gradient algorithm can be used to solve the inner convex subproblems [39]. Then, the convergence of fast gradient algorithm can be written as follows [39]:

$$\varrho_\tau^\iota = \mathcal{O}(1) \min \left\{ \sqrt{\frac{l_\iota}{\xi_\iota} \ln \left( \frac{l_\iota}{\tau} \right)}, \sqrt{\frac{l_\iota}{\xi_\iota}} \right\}, \iota = 1, 2, \quad (52)$$

where  $\tau$  is convergence tolerance.  $l_1$  and  $l_2$  are defined as the Lipschitz constants by which the Lipschitz conditions are satisfied with the gradients  $\nabla R_{buq,1}^{E,t}(\mathbf{p}, \mathbf{s})$  in subproblem (29) and (30), respectively. Moreover,  $\xi_1$  and  $\xi_2$  denote the convexity parameters to satisfy strong convexity of  $f_1$  and  $f_2$ , respectively. In other words, the fast gradient method is used to solve optimization problem (29) and (30) in  $\varrho_\tau^1$  and  $\varrho_\tau^2$  iterations, respectively. The iteration numbers  $\varrho_1$ ,  $\varrho_2$ , and  $\varrho_3$  are corresponding to the convergence tolerance  $\epsilon_1$ ,  $\epsilon_2$ , and  $\epsilon_3$  related to subalgorithms. Then, the overall computational complexity associated with the proposed algorithm is dominated by  $\varrho_1 \varrho_3 (\varrho_2 \varrho_\tau^1 + \varrho_2 \varrho_\tau^2)$ , where  $\varrho_2^1$  and  $\varrho_2^2$  are the iteration numbers of DC programming algorithm. The computational complexity of the proposed solution of the content placement problem is equal to  $\mathcal{O}(I_\theta B^{3.5} K^{3.5})$  [40] where  $I_\theta$  is the expected iteration numbers. The computational complexity of the our proposed MFCD problem is equal to  $\mathcal{O}(I_\beta F^{3.5} K^{3.5})$  [40] where  $I_\beta$  is the expected iteration numbers. The computational complexity of the proposed backhaul power and subcarrier

allocation problems are equal to  $\mathcal{O}(\hat{I}_{\tilde{p}}NFB \log_2(1/\epsilon_{\tilde{p}}))$  and  $\mathcal{O}(\hat{I}_{\zeta}NFB \log_2(1/\epsilon_{\zeta}))$  where  $\epsilon_{\tilde{p}}$ ,  $\hat{I}_{\tilde{p}}$ ,  $\epsilon_{\zeta}$  and  $\hat{I}_{\zeta}$  are the maximum error tolerance and expected iteration numbers, respectively.

## VI. SIMULATION RESULTS

For simulations, we consider a multi-cell downlink SCMA system where  $U$  users are randomly distributed in an area of circle with the radius of 1 km for each BS as the center. The number of users in circle area of  $b^{\text{th}}$  BS is set to  $U_b = 4, \forall b$ , and the total number of subcarriers and codebooks are set to 8 and 28, respectively. The bandwidth of each subcarrier is 180 kHz [41]. The channels between the MBS users and SBS users are generated with a normalized Rayleigh fading component and a distance-dependent path loss in urban and suburban areas, modeled as  $PL(dB) = 128.1 + 37.6 \log_{10}(d) + X$  and  $PL(dB) = 38 + 30 \log_{10}(d) + X$ , respectively [41], where  $d$  is the distance from user to BS in kilometres and  $X$  is 8 dB log-normal shadowing. We set the frame duration to  $T = 0.01$  s [42], [43]. The noise power  $(\sigma_u^n)^2 = (\sigma_b^n)^2 = \sigma^2, \forall u, b, n$  is set to  $-174$  dBm/Hz. We set  $D = 2$  and  $\eta_{nm} = 0.5, \forall n, m$  for SCMA [44]. We set the amount of harvested energy per arrival to  $\rho = 0.8$  Joules and  $\Gamma = 0.1$ . Simulation results are obtained by averaging over 1000 simulation runs.

### A. Effect of Maximum Allowable Backhaul Transmission Power

In this part, we obtain the backhaul rate for different values of backhaul transmission power with different values of  $\alpha$ . The simulation results are compared for different caching scenarios such as no caching, random caching, most popular caching and the proposed caching methods. In no caching case, no contents are stored by any BS. Hence, all the requested contents are served by core network over the backhaul links [45]–[47]. In random caching strategy, the contents are randomly cached by BSs until storage of BSs is full. Content popularity does not matter in this strategy. In the most popular caching strategy, each BS caches the most popular contents until its storage is full [45], [46]. The results are reported in Fig. 3(a). As can be seen, for a fixed transmit power, when  $\alpha$  is increased, the resulting backhaul rate increases. As can be seen from Fig. 3(a), utilizing the caching strategies can reduce backhaul traffic compared to the no caching scheme. It is also notable that most popular caching strategy causes more reduction in the backhaul traffic, compared to the random caching scheme. However, when all the caching placement are done jointly with the allocation of other network resources, the network performance increases

dramatically. This improvement is due to the fact that content placement is done according to network conditions and resources.

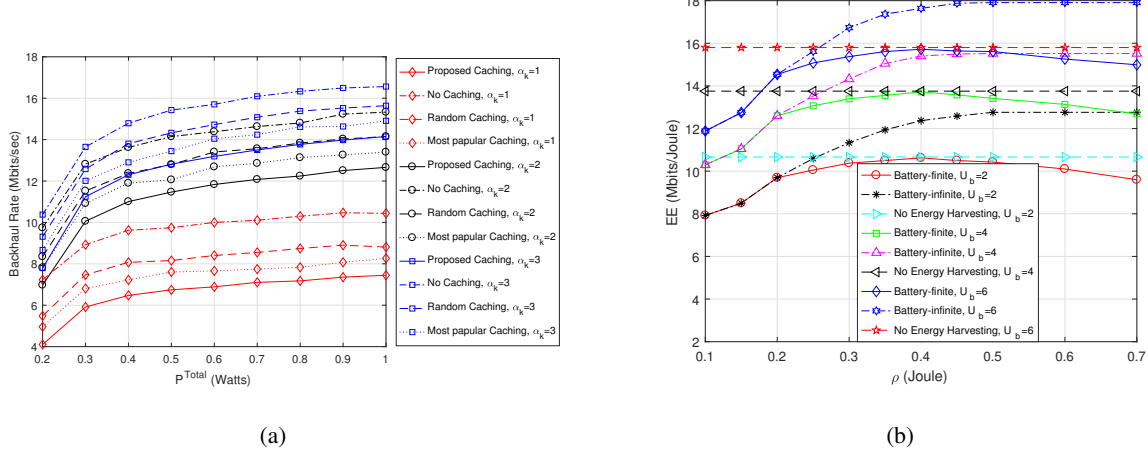


Fig. 3. (a) Backhaul rate,  $\tilde{R}$ , vs. the maximum backhaul transmit power constraint,  $\tilde{P}^{\text{Total}}$  for the SFCD scenario. System parameters are:  $B = 2, M = 28, F = 2, U = 4, N = 8, Q = 1, K = 6, D = 2, T = 0.01$  s,  $\forall k, V_b = 10$  Mbits,  $\forall b, E_b^{\text{max}} = 2$  Joule,  $\forall b, \rho = 0.5$  Joule,  $\varepsilon_h = 0.5$ . (b) Energy efficiency,  $EE$ , vs. the harvested energy per arrival,  $\rho$  for the SFCD scenario. System parameters are:  $B = 2, M = 28, F = 2, U = 2, N = 8, Q = 2, K = 6, D = 2, T = 0.01$  s,  $\alpha_k = 1$  Mbits,  $\forall k, V_b = 10$  Mbits,  $\forall b, \tilde{P}^{\text{Total}} = 0.1$  Watts,  $E_b^{\text{max}} = 2$  Joule,  $\forall b, \varepsilon_h = 0.5$ .

### B. Effect of Energy Harvesting

Fig. 3(b) shows the EE as a function of harvested energy per arrival,  $\rho$  for the SFCD scenario. We compare different EH strategy in term EE. In general, by increasing the EH value, the EE is also increased. For larger numbers of user, the EE is increased. In other words, for the small number of users, there is sufficient power resources, therefore by increasing users, the EE is also increased as shown in Fig. 3(b). However, for too more users, the power resource will be exhausted and thus some users can not access to network. Even so, due to multiuser diversity, the EE will still increase. For limited battery, due to overflow conditions (16), the stored energy must be used. Therefore, increasing the value of  $\rho$  will increase the energy efficiency at first, but with further increasing  $\rho$ , the energy efficiency decreases. However, for unlimited battery, with increasing  $\rho$ , the energy efficiency increases at first, and by further increasing the  $\rho$ , the energy efficiency becomes constant.

### C. Effect of File Splitting

Fig. 4(a) shows EE as a function of the harvested energy per arrival,  $\rho$  for the SFCD and MFCD scenarios. As can be seen from Fig. 3(b), the MFCD scheme outperforms the SFCD scenario. In the EE communication networks, due to random future of arrival energy, there may be not enough energy to transmit file that has big size in the SFCD scheme. In contrast, in the MFCD schemes, file is splitted into the several small size files which can be transmitted in the suitable frames to increase EE. In the uniform file splitting, the file is uniformly splitted into several smaller files with the same size. This scheme has better performance than the SFCD scheme. However, we can improve the network performance by using the our proposed method. In the our proposed MFCD scheme, the best size of each splitted file is obtained to enhance the network performance. This figure also shows that by reducing the size of file, the distance between the graphs for the three scenarios decreases.

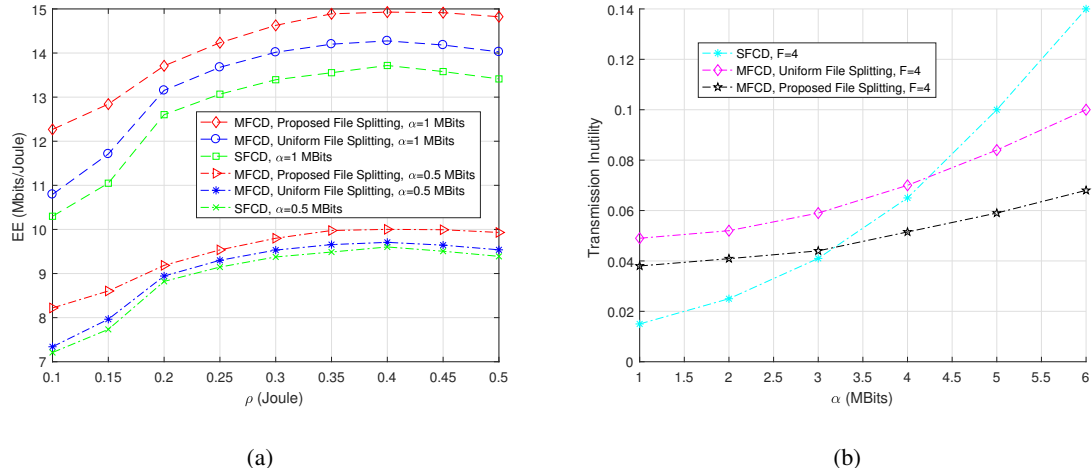


Fig. 4. (a) Energy efficiency,  $EE$ , vs. the harvested energy per arrival,  $\rho$ . System parameters are:  $B = 2, M = 28, F = 2, U = 2, N = 8, Q = 2, K = 6, D = 2, T = 0.01$  s,  $\forall b, V_b = 10$  Mbits,  $\forall b, \tilde{P}^{\text{Total}} = 0.1$  Watt,  $E_b^{\text{max}} = 2$  Joule,  $\forall b, \varepsilon_h = 0.5$ . (b) Outage probability, vs. the number of frames,  $F$ . System parameters are:  $B = 2, M = 28, U = 4, N = 8, Q = 2, K = 6, D = 2, T = 0.01$  s,  $V_b = 10$  Mbits,  $\forall b, \tilde{P}^{\text{Total}} = 1$  Watt,  $E_b^{\text{max}} = 2$  Joule,  $\forall b, \rho = 0.1$ , Joule,  $\varepsilon_h = 0.5$ .

### D. Transmission Inutility

In this section, we investigate the transmission inutility for SFCD and MFCD schemes. The transmission inutility is defined by multiplying the outage probability in the transmission delay. The outage probability is defined as probability that there is not enough battery to send content files and the transmission delay is defined as number of frames to sent files. Fig. 4(b) demonstrates

the transmission inutilities of our proposed schemes for different content file size. As can be seen, by increasing the size of file, the transmission inutility is increased for both schemes. This is due to the fact that there may be not enough harvested energy to sent file, and the energy deficiency probability can be increased. Therefore, the outage probability approaches to one in sufficiently big size of files. This deterioration in the MFCD schemes are less than the SFCD scheme. Because in the MFCD schemes, the deficiency probability of energy can be reduced by dividing the content file into several parts and sending each part in different frames. In the proposed splitting scheme, we find best fractional of content file for each frame which reduces the outage probability more than before. As shown in Fig. 4(b), for larger content file sizes, the MFCD scheme has a higher efficiency in reducing the outage probability. As can be seen, for the size of content files less than 3 MBits, SFCD scheme is better, while for the size of large files, the MFCD scheme is better.

### E. Effect of Channel Uncertainty

Fig. 5(a) shows EE, secrecy access and backhual rate versus channel uncertainty for the SFCD scenario. We see that at bigger channel uncertainty, the secrecy access rate clearly have low value. As can be seen in Fig. 5(a), as the number of eavesdroppers increases, the secrecy access rate decreases significantly.

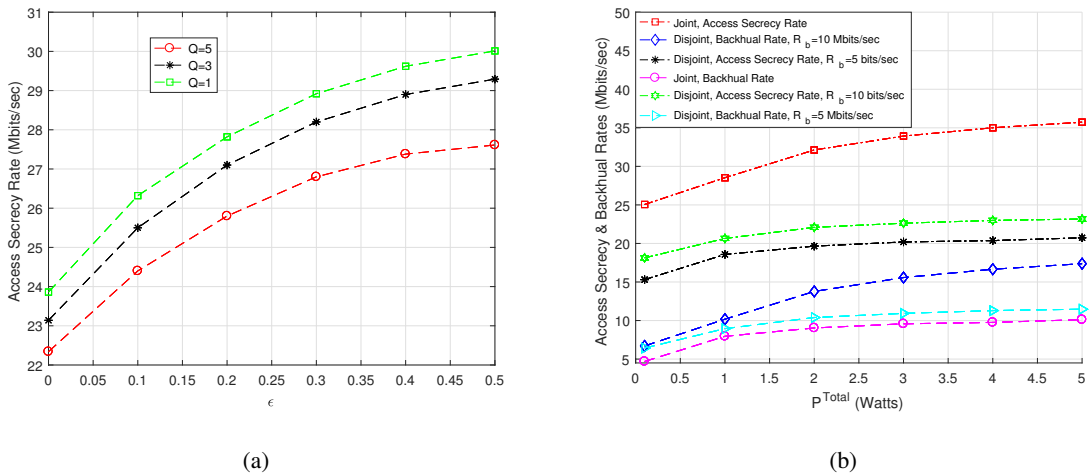


Fig. 5. (a) EE, secrecy access and backhual rate,  $R^S$ , vs. the channel uncertainty,  $\epsilon_h$  for the SFCD scenario. System parameters are:  $B = 2, M = 28, F = 2, U = 2, N = 8, Q = 1, K = 6, D = 2, T = 0.01$  s,  $\alpha_k = 1$  Mbits,  $\forall k, V_b = 10$  Mbits,  $\tilde{P}^{\text{Total}} = 0.1$  Watt,  $E_b^{\text{max}} = 2$  Joule,  $\forall b, \rho = 0.5$  Joule. (b) Secrecy access and backhual rates,  $R^S$  and  $\tilde{R}$ , vs. the backhaul transmission power,  $P^{\text{Total}}$  for the SFCD scenario. System parameters are:  $B = 2, M = 28, F = 2, U = 4, N = 8, Q = 1, K = 6, D = 2, T = 0.01$  s,  $\alpha_k = 1$  Mbits,  $\forall k, V_b = 10$  Mbits,  $\forall b, E_b^{\text{max}} = 5$  Joule,  $\forall b, \rho = 0.5$  Joule,  $\epsilon_h = 0.5$ .

#### *F. Comparison Between Joint backhaul and access optimization and Disjoint Optimization Problem Solution*

Fig. 5(b) illustrates the comparison between joint optimization and disjoint optimization problem solution versus different backhaul transmission power for the SFCD scenario. In solving the main problem disjointly, access and backhaul optimization problems are resolved separately. In the other words, first, the backhaul problem is solved with respect to the threshold for the access secrecy rate, and then the access problem is solved. It can be noticed that the joint backhaul and access optimization problem approaches better solution than disjoint backhaul and access optimization problem. Also notice that the backhual rate of joint backhual and access optimization problem scheme increases with increasing access link rate threshold,  $R_b$ .

#### *G. Effect of super frame size*

Fig. 6(a) shows the variation of the EE, secrecy access rate with the number of frames,  $F$  for the SFCD scenario. As shown in Fig. 6(a) by increasing super frame size, the secrecy access rate increases. In the other words, by increasing super frame size, the transmitter can transmit data stream over different frames, then the secrecy access rate and EE will increase. For limited battery storage, with increasing super frame size, at first the EE increases. However, with further increasing super frame size, due to energy overflow constraints (16) which enforce the transmitters to spend energy, the energy efficiency decreases. Note that, as the value of  $\alpha$  becomes larger, this effect happens in lower super frame size. For unlimited battery storage, since the overflow constrains (16) are absent, all the harvested energy is stored in the battery. In this case, increasing super frame size will increase the diversity gain, and hence, the energy efficiency increases.

#### *H. The Convergence of the Proposed Algorithm*

In this part, we investigate the performance of the proposed resource allocation algorithm. In Fig. 6(b), we show obtaining EE after each iteration at the proposed alternate optimization algorithm. As can be seen in Fig. 6(b), the convergence of the proposed algorithm can averagely be achieved within 700 iterations.

## VII. CONCLUSION

In this paper, we provided a unified framework for radio resources allocation and content placement considering the physical layer security and the channel uncertainty to provide higher

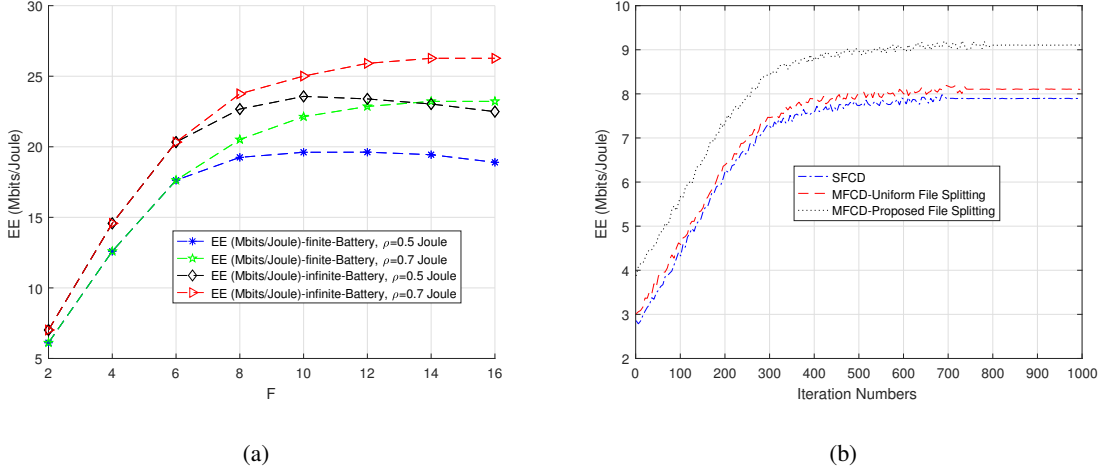


Fig. 6. (a) EE, secrecy access rate, vs. the super frame size,  $F$ . System parameters are:  $B = 2, M = 28, U = 4, N = 8, Q = 1, K = 6, D = 2, T = 0.01$  s,  $\alpha_k = 1$  Mbits,  $\forall k, V_b = 10$  Mbits,  $\forall b, E_b^{\max} = 5$  Joule,  $\forall b, \rho = 0.5$  Joule,  $\varepsilon_h = 0.5$ . (b) Energy efficiency, EE, vs. the iteration number. System parameters are:  $B = 2, M = 28, F = 2, U = 2, N = 8, Q = 1, K = 6, D = 2, T = 0.01$  s,  $\alpha_k = 1$  Mbits,  $\forall k, V_b = 10$  Mbits,  $\forall b, \tilde{P}^{\text{Total}} = 0.1$  Watt,  $\rho = 0.1$  Joule,  $E_b^{\max} = 2$  Joule,  $\forall b, \varepsilon_h = 0.5$ .

energy efficiency. To do so, we considered downlink SCMA scenarios, and we aimed at maximizing the worst case energy efficiency subject to system constraints which determines the radio resources allocation and content placement parameter. Moreover, we proposed two novel content delivery scenarios: 1) single frame content delivery, and 2) multiple frames content delivery. In the first scenario, the requested content by each user is served over one frame. However, in the second scenario, the requested content by each user can be delivered over several frames. Since the optimization problems are nonconvex and NP-hard, we provided an iterative method converging to a local solution. Finally, we showed the resulting secrecy access rate, backhaul rate, and energy efficiency for different values of maximum backhaul transmit power as well as different number of users and various content size. In addition, we compared the performance of the proposed caching scheme with the existing traditional caching schemes. Based on simulation results, via our proposed caching scheme, the performance is approximately improved by 14% and 21% compared to the most popular and random caching schemes, respectively. Moreover, it can be seen that the MFCD scheme can approximately enhance the system performance by 5.2% and 11.1% for small and large files, respectively.

## APPENDIX A

### PROOF OF THEOREM 1

In accordance to the foregoing discussions, for (28) with a given  $\mathbf{e}_{h\varrho}$ ,  $(\mathbf{p}_{\varrho+1}, \tilde{\mathbf{p}}_{\varrho+1}, \mathbf{s}_{\varrho+1}, \boldsymbol{\theta}_{\varrho+1}, \boldsymbol{\zeta}_{\varrho+1})$  is its optimal solution, while  $(\mathbf{p}_\varrho, \tilde{\mathbf{p}}_\varrho, \mathbf{s}_\varrho, \boldsymbol{\theta}_\varrho, \boldsymbol{\zeta}_\varrho)$  is only its feasible solution. We get that

$$\Xi_{EE}(\mathbf{p}_{\varrho+1}, \tilde{\mathbf{p}}_{\varrho+1}, \mathbf{s}_{\varrho+1}, \boldsymbol{\theta}_{\varrho+1}, \boldsymbol{\zeta}_{\varrho+1}, \mathbf{e}_{h\varrho}) \leq \Xi_{EE}(\mathbf{p}_\varrho, \tilde{\mathbf{p}}_\varrho, \mathbf{s}_\varrho, \boldsymbol{\theta}_\varrho, \boldsymbol{\zeta}_\varrho, \mathbf{e}_{h\varrho}). \quad (53)$$

Likewise, for (29) with a given  $\mathbf{p}_\varrho$ ,  $(\tilde{\mathbf{p}}_{\varrho+1}, \mathbf{s}_{\varrho+1}, \boldsymbol{\theta}_{\varrho+1}, \boldsymbol{\zeta}_{\varrho+1}, \mathbf{e}_{h\varrho+1})$  is its optimal solution, while  $(\tilde{\mathbf{p}}_\varrho, \mathbf{s}_\varrho, \boldsymbol{\theta}_\varrho, \boldsymbol{\zeta}_\varrho, \mathbf{e}_{h\varrho})$  is only its feasible solution. It follows that

$$\Xi_{EE}(\mathbf{p}_\varrho, \tilde{\mathbf{p}}_{\varrho+1}, \mathbf{s}_{\varrho+1}, \boldsymbol{\theta}_{\varrho+1}, \boldsymbol{\zeta}_{\varrho+1}, \mathbf{e}_{h\varrho+1}) \leq \Xi_{EE}(\mathbf{p}_\varrho, \tilde{\mathbf{p}}_\varrho, \mathbf{s}_\varrho, \boldsymbol{\theta}_\varrho, \boldsymbol{\zeta}_\varrho, \mathbf{e}_{h\varrho}). \quad (54)$$

For relations (30), (31), (32) and (33), this trend is similar. It is naturally concluded that

$$\Xi_{EE}(\mathbf{p}_{\varrho+1}, \tilde{\mathbf{p}}_{\varrho+1}, \mathbf{s}_{\varrho+1}, \boldsymbol{\theta}_{\varrho+1}, \boldsymbol{\zeta}_{\varrho+1}, \mathbf{e}_{h\varrho+1}) \leq \Xi_{EE}(\mathbf{p}_\varrho, \tilde{\mathbf{p}}_\varrho, \mathbf{s}_\varrho, \boldsymbol{\theta}_\varrho, \boldsymbol{\zeta}_\varrho, \mathbf{e}_{h\varrho}). \quad (55)$$

## APPENDIX B

### PROOF OF THEOREM 2

Because of the convexity of  $R_{buq1}^{E,mt}$ , it follows that

$$R_{buq1}^{E,mt}(\varrho+1) \geq R_{buq1}^{E,mt}(\varrho) - \left\langle \nabla R_{bu1}^{E,t}(\varrho), p_{bu}^{mt}(\varrho+1) - p_{bu}^{mt}(\varrho) \right\rangle, \quad (56)$$

for  $p_{bu}^{mt}(\varrho)$  and  $p_{bu}^{mt}(\varrho+1)$  in the feasible domain. We can deduce that

$$-(R_{buq2}^{E,mt}(\varrho+1) - R_{buq1}^{E,mt}(\varrho) - \left\langle \nabla R_{bu1}^{E,t}(\varrho), p_{bu}^{mt}(\varrho+1) - p_{bu}^{mt}(\varrho) \right\rangle) \leq -(R_{buq2}^{E,mt}(\varrho) - R_{buq1}^{E,mt}(\varrho)), \quad (57)$$

Combined with (56) and (57), we conclude that

$$-(R_{buq2}^{E,mt}(\varrho+1) - R_{buq1}^{E,mt}(\varrho+1)) \leq -(R_{buq2}^{E,mt}(\varrho) - R_{buq1}^{E,mt}(\varrho)). \quad (58)$$

Obviously, the current value  $R_{buq}^{E,mt}(\varrho+1)$  is smaller than the previous value  $R_{buq}^{E,mt}(\varrho)$  while the current solution  $p_{bu}^{mt}(\varrho+1)$  is better than the previous solution  $p_{bu}^{mt}(\varrho)$ . As a result, the theorem is proved.

## REFERENCES

- [1] S. Woo, E. Jeong, S. Park, J. Lee, S. Ihm, and K. Park, “Comparison of caching strategies in modern cellular backhaul networks,” in *Proceeding of the 11th annual international conference on Mobile systems, applications, and services*, New York, NY, USA, June 2013, pp. 319–332.
- [2] E. Bastug, M. Bennis, and M. Debbah, “Living on the edge: The role of proactive caching in 5G wireless networks,” *IEEE Communications Magazine*, vol. 52, no. 8, pp. 82–89, August 2014.
- [3] H. Ahlehagh and S. Dey, “Video-aware scheduling and caching in the radio access network,” *IEEE/ACM Transactions on Networking (TON)*, vol. 22, no. 5, pp. 1444–1462, 2014.
- [4] K. Shanmugam, N. Golrezaei, A. G. Dimakis, A. F. Molisch, and G. Caire, “Femtocaching: Wireless content delivery through distributed caching helpers,” *IEEE Transactions on Information Theory*, vol. 59, no. 12, pp. 8402–8413, 2013.
- [5] N. Golrezaei, A. F. Molisch, A. G. Dimakis, and G. Caire, “Femtocaching and device-to-device collaboration: A new architecture for wireless video distribution,” *IEEE Communications Magazine*, vol. 51, no. 4, pp. 142–149, 2013.
- [6] E. M. Yeatman, “Advances in power sources for wireless sensor nodes,” in *Proceeding of Intl Workshop on Wearable and Implantable Body Sensor Networks*, London, United Kingdom, July 2004, pp. 20–21.
- [7] J. A. Paradiso and T. Starner, “Energy scavenging for mobile and wireless electronics,” *IEEE Pervasive Computing*, vol. 12, no. 4, pp. 18–27, January 2005.
- [8] N. Hosein and B. Hadi, “Sparse code multiple access,” in *Proceedings of IEEE 24th Annual International Symposium on Personal, Indoor, and Mobile Radio Communications (PIMRC)*, London, UK, September 2013, pp. 332–336.
- [9] K. Au, a. H. N. L. Zhang, A. B. E. Yi, U. Vilaipornsawai, J. Ma, and P. Zhu, “Uplink contention based SCMA for 5G radio access,” in *Proceeding of IEEE GLOBECOM14*, Texas, USA, December 2014, pp. 900–905.
- [10] Z. Li, W. Chen, F. Wei, F. Wang, X. Xu, and Y. Chen, “Joint codebook assignment and power allocation for SCMA based on capacity with gaussian input,” in *Communications in China (ICCC), 2016 IEEE/CIC International Conference on*. IEEE, 2016, pp. 1–6.
- [11] Y. Li, M. Sheng, Z. Sun, Y. Sun, L. Liu, D. Zhai, and J. Li, “Cost-efficient codebook assignment and power allocation for energy efficiency maximization in SCMA networks,” in *Vehicular Technology Conference (VTC-Fall), 2016 IEEE 84th*. IEEE, 2016, pp. 1–5.
- [12] N. Ahmed, M. A. Khojastepour, A. Sabharwal, and B. Aazhang, “Outage minimization with limited feedback for the fading relay channel,” *IEEE Transactions on Communications*, vol. 54, no. 4, pp. 659–669, 2006.
- [13] N. Mokari, F. Alavi, S. Parsaeefard, and T. Le-Ngoc, “Limited-feedback resource allocation in heterogeneous cellular networks,” *IEEE Transactions on Vehicular Technology*, vol. 65, no. 4, pp. 2509–2521, 2016.
- [14] M. R. Javan, N. Mokari, F. Alavi, and A. Rahmati, “Resource allocation in decode-and-forward cooperative communication networks with limited rate feedback channel,” *IEEE Transactions on Vehicular Technology*, vol. 66, no. 1, pp. 256–267, 2017.
- [15] I. Csiszár and P. Narayan, “Secrecy generation for multiaccess channel models,” *IEEE Transactions on Information Theory*, vol. 59, no. 1, pp. 17–31, 2013.
- [16] A. D. Wyner, “The wire-tap channel,” *Bell Labs Technical Journal*, vol. 54, no. 8, pp. 1355–1387, 1975.
- [17] F. Alavi, N. M. YAMCHI, M. R. Javan, and K. Cumanan, “Limited feedback scheme for device to device communications in 5G cellular networks with reliability and cellular secrecy outage constraints,” *IEEE Transactions on Vehicular Technology*, 2017.
- [18] M. R. Abedi, N. Mokari, M. R. Javan, and H. Yanikomeroglu, “Limited rate feedback scheme for resource allocation in

secure relay-assisted OFDMA networks,” *IEEE Transactions on Wireless Communications*, vol. 15, no. 4, pp. 2604–2618, 2016.

[19] L. Wang, K.-K. Wong, S. Jin, G. Zheng, and R. W. Heath Jr, “A new look at physical layer security, caching, and wireless energy harvesting for heterogeneous ultra-dense networks,” *arXiv preprint arXiv:1705.09647*, 2017.

[20] A. Sharma, R. K. Ganti, and J. K. Millett, “Joint backhaul-access analysis of full duplex self-backhauling heterogeneous networks,” *IEEE Transactions on Wireless Communications*, vol. 16, no. 3, pp. 1727–1740, 2017.

[21] O. Dhifallah, H. Dahrouj, T. Y. Al-Naffouri, and M.-S. Alouini, “Joint hybrid backhaul and access links design in cloud-radio access networks,” in *Vehicular Technology Conference (VTC Fall), 2015 IEEE 82nd*. IEEE, 2015, pp. 1–5.

[22] C. Hua, Y. Luo, and H. Liu, “Wireless backhaul resource allocation and user-centric clustering in ultra-dense wireless networks,” *IET Communications*, vol. 10, no. 15, pp. 1858–1864, 2016.

[23] M. Shariat, E. Pateromichelakis, A. ul Quddus, and R. Tafazolli, “Joint TDD backhaul and access optimization in dense small-cell networks,” *IEEE Transactions on Vehicular Technology*, vol. 64, no. 11, pp. 5288–5299, 2015.

[24] H. Zhuang, J. Chen, and D. O. Wu, “Joint access and backhaul resource management for ultra-dense networks,” in *Communications (ICC), 2017 IEEE International Conference on*. IEEE, 2017, pp. 1–6.

[25] M. Mirahsan, H. Farmanbar, and H. Yanikomeroglu, “Joint backhaul and access optimization for service-segment-based VN admission control.”

[26] Y. Niu, C. Gao, Y. Li, L. Su, D. Jin, and A. V. Vasilakos, “Exploiting device-to-device communications in joint scheduling of access and backhaul for mmwave small cells,” *IEEE Journal on Selected Areas in Communications*, vol. 33, no. 10, pp. 2052–2069, 2015.

[27] “Spectrum and technology issues for microwave backhaul in europe,” Innovation Observatory Ltd, Silvaco Technology Centre, Compass Point Business Park, St Ives, Cambs., PE27 5JL, UK, Tech. Rep., November 2010.

[28] R. Hoshyar, F. Wathan, and R. Tafazolli, “Novel low-density signature for synchronous CDMA systems over AWGN channel,” *IEEE Transactions on Signal Processing*, vol. 56, no. 4, pp. 1616–1626, April 2008.

[29] Y. Luo, J. Zhang, and K. B. Letaief, “Optimal scheduling and power allocation for two-hop energy harvesting communication systems,” *IEEE Transactions on Wireless Communications*, vol. 12, no. 9, pp. 4729–4741, 2013.

[30] A. Minasian, S. ShahbazPanahi, and R. S. Adve, “Energy harvesting cooperative communication systems,” *IEEE Transactions on Wireless Communications*, vol. 13, no. 11, pp. 6118–6131, 2014.

[31] P. Sobkowicz, M. Thelwall, K. Buckley, G. Paltoglou, and A. Sobkowicz, “Lognormal distributions of user post lengths in internet discussions-a consequence of the weber-fechner law?” *EPJ Data Science*, vol. 2, no. 1, p. 2, 2013.

[32] O. Ozel, K. Tutuncuoglu, J. Yang, S. Ulukus, and A. Yener, “Transmission with energy harvesting nodes in fading wireless channels: Optimal policies,” *IEEE Journal on Selected Areas in Communications*, vol. 29, no. 8, pp. 1732–1743, 2011.

[33] H. S. Dhillon, Y. Li, P. Nuggehalli, Z. Pi, and J. G. Andrews, “Fundamentals of heterogeneous cellular networks with energy harvesting,” *IEEE Transactions on Wireless Communications*, vol. 13, no. 5, pp. 2782–2797, 2014.

[34] S. Boyd and L. Vandenberghe, *Convex optimization*. Cambridge university press, 2004.

[35] N.-T. Le, T. Van Do, N. T. Nguyen, and H. A. Le Thi, “Advanced computational methods for knowledge engineering,” 2013.

[36] G. Michael, B. Stephen, and Y. Y. CvX, “Matlab software for disciplined convex programming, version 2.0 beta,” *Recent Advances in Learning and Control*, pp. 95–110, 2012.

[37] W. Dinkelbach, “On nonlinear fractional programming,” *Management Science*, vol. 13, no. 4, pp. 492–498, March 1967.

[38] S. Schaible, “Fractional programming. ii, on dinkelbachs algorithm,” *Management Science*, vol. 22, no. 8, pp. 868–873, April 1976.

- [39] S. Richter, C. N. Jones, and M. Morari, “Computational complexity certification for real-time MPC with input constraints based on the fast gradient method,” *IEEE Transactions on Automatic Control*, vol. 57, no. 6, pp. 1391–1403, 2012.
- [40] A. Ben-Tal and A. Nemirovski, *Lectures on modern convex optimization: analysis, algorithms, and engineering applications*. SIAM, 2001.
- [41] T. ETSI, “136 931 v9. 0.0,LTE; evolved universal terrestrial radio access (E-UTRA); radio frequency (RF) requirements for LTE pico node B,” 3GPP TR 36.931 version 9.0. 0 Release 9), 2011. Online at: [http://www.etsi.org/deliver/etsi\\_ts/136100\\_136199/13610\\_4/09.04.00\\_60/ts\\_136104v090400p.pdf](http://www.etsi.org/deliver/etsi_ts/136100_136199/13610_4/09.04.00_60/ts_136104v090400p.pdf), Tech. Rep., 2011.
- [42] P. Castiglione and G. Matz, “Energy-neutral source-channel coding with battery and memory size constraints,” *IEEE Transactions on Communications*, vol. 62, no. 4, pp. 1373–1381, 2014.
- [43] F. Zhang and V. K. Lau, “Delay-sensitive dynamic resource control for energy harvesting wireless systems with finite energy storage,” *IEEE Communications Magazine*, vol. 53, no. 8, pp. 106–113, 2015.
- [44] H. Nikopour and H. Baligh, “Sparse code multiple access,” in *Personal Indoor and Mobile Radio Communications (PIMRC), 2013 IEEE 24th International Symposium on*. IEEE, 2013, pp. 332–336.
- [45] S.-H. Park, O. Simeone, and S. S. Shitz, “Joint optimization of cloud and edge processing for fog radio access networks,” *IEEE Transactions on Wireless Communications*, vol. 15, no. 11, pp. 7621–7632, 2016.
- [46] R. G. Stephen and R. Zhang, “Green OFDMA resource allocation in cache-enabled CRAN,” in *Green Communications (OnlineGreenComm), 2016 IEEE Online Conference on*. IEEE, 2016, pp. 70–75.
- [47] H. Hsu and K.-C. Chen, “A resource allocation perspective on caching to achieve low latency,” *IEEE Communications Letters*, vol. 20, no. 1, pp. 145–148, 2016.